

Robust Discrete Pricing Optimization via Multiple-Choice Knapsack Reductions

Zi Yuan Eric Shao¹

¹*Department of Mathematics, ETH Zürich, ershao@student.ethz.ch*

March 2026

We study a discrete portfolio pricing problem that selects one price per product from a finite menu under margin and fairness constraints. To account for demand uncertainty, we incorporate a budgeted robust formulation that controls conservatism while remaining computationally tractable. By reducing the problem to a Multiple-Choice Knapsack Problem (MCKP), we identify structural properties of the LP relaxation—in particular, upper-hull filtering and greedy filling over hull segments—that yield an exact solution method for the LP relaxation of the fixed-parameter subproblems. For the resulting fixed-parameter subproblems, we show that the integrality gap is bounded additively by a single-item hull jump, and that the corresponding relative gap decays as $O(1/n)$ under standard boundedness and linear-growth assumptions. Numerical experiments on synthetic portfolios and a stylized retail case study with economically calibrated parameters are consistent with these bounds and indicate that robust margin protection can be achieved with less than 1% nominal revenue loss on the instances tested.

Keywords: Discrete Optimization; Robust Optimization; Pricing; Knapsack Problem

1 Introduction and Reduction

We consider a pricing optimization problem where a decision maker must set prices for a collection of items in order to maximize overall value (e.g., profit or revenue), subject to two key constraints. First, the portfolio must achieve at least a prescribed margin level, so that overall profitability remains acceptable. Second, each individual price must stay sufficiently close to a given reference or “fair” price, reflecting regulatory, actuarial, or market considerations. Problems of this type arise repeatedly in practice, for instance in insurance tariff setting, retail and e-commerce pricing, or energy and telecom tariffs, whenever large price menus must be adjusted under margin and fairness constraints.

Two modeling choices deserve brief justification. We work with *discrete* price menus because many applied settings (e.g., insurance tariffs, retail shelf prices with psychological endings, and standardized energy contracts) restrict the decision maker to a finite set of admissible price points, and continuous relaxations can therefore produce infeasible prices. We also impose the margin requirement as a *ratio* constraint $N(\mathbf{x})/D(\mathbf{x}) \geq \Delta$ rather than an additive floor $N(\mathbf{x}) - D(\mathbf{x}) \geq b$. The ratio form is scale-invariant and matches standard profitability metrics such as loss ratio and gross-margin percentage.

Contributions. Our contributions are threefold.

- (i) We formulate a discrete portfolio pricing problem with ratio-based margin and fairness constraints and show that it reduces *exactly* to a Multiple-Choice Knapsack Problem (MCKP). While the MCKP is classical, the reduction from constrained pricing with ratio margins, fairness bands, and weighted demand provides a direct bridge between pricing practice and combinatorial optimization theory.
- (ii) We introduce a Γ -budget robust extension of this MCKP and prove that the coupled robust constraint admits a *parametric dual decomposition* ([Theorem 6](#)) that reduces the problem to a one-dimensional enumeration over a finite breakpoint set ([Proposition 7](#)). This yields a specialized structure-exploiting algorithmic framework for the Γ -budget robust MCKP that avoids relying on a generic MILP reformulation inside the main solution loop.

- (iii) We establish that the integrality gap of each fixed- θ subproblem is bounded additively by a single item's maximum hull-value jump ΔV_{\max}^{θ} (Proposition 9), yielding a relative gap of $O(1/n)$ for large portfolios (Corollary 10). Numerical experiments on synthetic and economically calibrated instances are consistent with these bounds and indicate that robust margin protection costs less than 1% of nominal revenue on the instances tested.

The LP relaxation analysis in Section 4 (Theorem 5) consolidates known MCKP relaxation properties (Dyer, 1984; Pisinger, 1995) and is re-proved in a self-contained way in our notation. The main novelty lies in contributions (ii) and (iii) and in the end-to-end pipeline connecting the pricing formulation to a specialized robust optimization procedure built around hull-based LP structure.

1.1 Problem Formulation

Mathematically we have the following discrete problem. For each class $i \in \{1, \dots, n\}$, we choose one price level $x_i \in \mathcal{X}_i = \{x_{i,1}, \dots, x_{i,m}\}$. We are given parameters for each class i : reference price $a_i > 0$, weight exposure ω_i , nominal demand $\hat{g}_i : \mathcal{X}_i \rightarrow \mathbb{R}_{\geq 0}$ (monotone decreasing on the admissible range; e.g. piecewise-linear or iso-elastic), relative tolerance σ_i , and a margin target parameter $\Delta > 0$. We assume the demand functions \hat{g}_i depend only on the own-price x_i and not on other items' prices, which is appropriate when cross-product substitution is negligible (see Section 8 for extensions).

Define:

$$N(\mathbf{x}) := \sum_{i=1}^n \omega_i x_i \hat{g}_i(x_i), \quad D(\mathbf{x}) := \sum_{i=1}^n \omega_i a_i \hat{g}_i(x_i) > 0, \quad S(\mathbf{x}) := N(\mathbf{x}) - \Delta \cdot D(\mathbf{x}).$$

Optimization Problem:

$$\max_{\mathbf{x}} \quad N(\mathbf{x}) = \sum_{i=1}^n \omega_i x_i \hat{g}_i(x_i), \quad (1)$$

$$\text{s. t.} \quad \frac{N(\mathbf{x})}{D(\mathbf{x})} \geq \Delta \Leftrightarrow S(\mathbf{x}) \geq 0, \quad (2)$$

$$\frac{|x_i - a_i|}{a_i} \leq \sigma_i \iff x_i \in [(1 - \sigma_i)a_i, (1 + \sigma_i)a_i] \quad (\forall i). \quad (3)$$

The second constraint can be easily mitigated by defining the admissible menu

$$I_i := [(1 - \sigma_i)a_i, (1 + \sigma_i)a_i], \quad \mathcal{X}_i^{\text{ad}} := \mathcal{X}_i \cap I_i \neq \emptyset, \quad i = 1, \dots, n,$$

and henceforth restrict all decisions to $x_i \in \mathcal{X}_i^{\text{ad}}$.

1.2 Reduction to MCKP

For a formal introduction to the classical 0–1 Knapsack problem and the standard MCKP definition, we refer to Section A. Introduce binary selection variables $z_{ij} \in \{0, 1\}$ indicating the choice $x_i = x_{i,j}$. For each option $x_{i,j} \in \mathcal{X}_i$, define

$$v_{ij} := \omega_i x_{i,j} \hat{g}_i(x_{i,j}), \quad (4)$$

$$d_{ij} := \omega_i a_i \hat{g}_i(x_{i,j}), \quad (5)$$

$$s_{ij} := v_{ij} - \Delta d_{ij}. \quad (6)$$

Let $J_i^{\text{ad}} := \{j \in \{1, \dots, m\} : x_{i,j} \in \mathcal{X}_i^{\text{ad}}\}$ denote the admissible indices. Then

$$N(\mathbf{x}) = \sum_{i=1}^n \sum_{j \in J_i^{\text{ad}}} v_{ij} z_{ij}, \quad S(\mathbf{x}) = \sum_{i=1}^n \sum_{j \in J_i^{\text{ad}}} s_{ij} z_{ij}, \quad \sum_{j \in J_i^{\text{ad}}} z_{ij} = 1 \quad (\forall i).$$

To obtain a single knapsack constraint with nonnegative costs, apply a baseline–slack transformation. For each i choose a baseline option

$$\begin{aligned} j^*(i) &\in \arg \max_{j \in J_i^{\text{ad}}} s_{ij}, \\ S_{\max} &:= \sum_{i=1}^n s_{i j^*(i)}, \\ c_{ij} &:= s_{i j^*(i)} - s_{ij} \quad (\geq 0) \quad (j \in J_i^{\text{ad}}). \end{aligned}$$

Then

$$\sum_{i=1}^n \sum_{j \in J_i^{\text{ad}}} s_{ij} z_{ij} = \sum_{i=1}^n s_{i j^*(i)} - \sum_{i=1}^n \sum_{j \in J_i^{\text{ad}}} c_{ij} z_{ij} = S_{\max} - \sum_{i=1}^n \sum_{j \in J_i^{\text{ad}}} c_{ij} z_{ij}.$$

Hence the ratio constraint $S(\mathbf{x}) \geq 0$ is equivalent to the knapsack inequality

$$\sum_{i=1}^n \sum_{j \in J_i^{\text{ad}}} c_{ij} z_{ij} \leq S_{\max}.$$

The pricing problem is therefore exactly the multiple-choice knapsack problem (MCKP)

$$\max \sum_{i=1}^n \sum_{j \in J_i^{\text{ad}}} v_{ij} z_{ij} \tag{7}$$

$$\text{s.t.} \quad \sum_{i=1}^n \sum_{j \in J_i^{\text{ad}}} c_{ij} z_{ij} \leq S_{\max}, \tag{8}$$

$$\sum_{j \in J_i^{\text{ad}}} z_{ij} = 1 \quad (i = 1, \dots, n), \tag{9}$$

$$z_{ij} \in \{0, 1\} \quad (\forall i, j \in J_i^{\text{ad}}). \tag{10}$$

2 Related Work

MCKP foundations. The Multiple-Choice Knapsack Problem (MCKP) is a classical discrete optimization model in which exactly one option is selected from each of n groups under a knapsack constraint. Early work established NP-hardness and developed exact methods based on branch-and-bound and dominance preprocessing; see, e.g., [Nauss \(1978\)](#); [Ibaraki et al. \(1978\)](#); [Sinha and Zoltner \(1979\)](#). A key structural feature is the near-integrality of the LP relaxation: there exists an optimal LP solution in which all but at most one group choose a single option, while one group (at most) is mixed between two options ([Dyer, 1984](#)). This LP structure underpins many exact and heuristic schemes and is closely related to convex-hull and “core” ideas used in practical solvers ([Pisinger, 1995](#); [Kellerer et al., 2004](#)).

Extensions and uncertainty. Motivated by applications in large-scale pricing and resource allocation, recent work has considered generalizations such as setup decisions and additional side constraints, where decomposition and matheuristics become effective (e.g., [Boukhari and Hifi, 2023, 2024](#)). In parallel, uncertainty in demand and cost parameters has renewed interest in approaches beyond purely stochastic models, which often require distributional information that is unavailable or unreliable. Robust Optimization (RO) provides an attractive alternative ([Ben-Tal and Nemirovski, 1999](#)), and the budgeted uncertainty model of [Bertsimas and Sim \(2004\)](#) (Γ -robustness) controls the trade-off between conservatism and performance while preserving tractability properties for many linear problems. Recent applications have illustrated the value of this approach in multi-product pricing under interval uncertainties ([Hamzei et al., 2022](#)).

Gap addressed in this paper. For knapsack-type problems, exact and combinatorial algorithms for robust variants are well studied in the single-choice setting (e.g., [Monaci et al., 2013](#)). In contrast, the multiple-choice setting with Γ -budget coupling has received comparatively less attention in terms of specialized, structure-exploiting algorithms. The formulation of [Caserta and Voß \(2019\)](#) relies on a generic MILP reformulation of the robust constraints together with kernel-search-style matheuristics, without exploiting the MCKP’s upper-hull LP structure. Extensions such as locally budgeted uncertainty further enrich modeling flexibility ([Goerigk et al., 2021](#)), but these formulations are typically validated through general-purpose solvers rather than structure-specific algorithms. The present paper exploits the convex-hull LP structure of the MCKP *within* a Γ -budget robust framework, yielding a specialized algorithmic approach with provable integrality-gap bounds. The pricing reduction of [Section 1](#) provides the applied motivation; the structural and algorithmic results ([Sections 4](#) and [5](#)) apply to any MCKP with Γ -budget uncertainty in the capacity constraint, independent of the pricing interpretation.

3 Robust Pricing under Demand Uncertainty

In the formulation presented in [Section 1](#), the demand response $\hat{g}_i(x_i)$ is treated as a deterministic function of price even though demand estimates are subject to statistical error. To mitigate this risk, we introduce a **Budgeted Robust** framework in which the true demand $\tilde{g}_i(x_i)$ resides in an uncertainty set \mathcal{U} and the margin constraint must hold for *all* realizations in that set. We then seek a price vector \mathbf{x} that maximizes nominal revenue subject to this worst-case feasibility requirement.

3.1 Uncertainty Model

We assume the realized demand lies within a symmetric interval around the nominal value:

$$\tilde{g}_i(x_i) \in [\hat{g}_i(x_i) - \delta_i(x_i), \hat{g}_i(x_i) + \delta_i(x_i)], \quad (11)$$

where $\delta_i(x_i) \geq 0$ is a variability parameter (e.g., derived from the standard error of the demand estimation). We assume $\delta_i(x_i) \leq \hat{g}_i(x_i)$ on $\mathcal{X}_i^{\text{ad}}$, so demand remains nonnegative under uncertainty.

To avoid overly conservative solutions—such as those arising from box uncertainty where every product realizes its worst-case simultaneously—we adopt the “Budget of Uncertainty” approach proposed by [Bertsimas and Sim \(2004\)](#). We define an integer budget $\Gamma \in \{0, 1, \dots, n\}$, representing the maximum number of products that can simultaneously deviate to their worst-case limits.

Definition 1 (Uncertainty Set). Let $\xi_i \in [-1, 1]$ be the scaled deviation for item i . For a fixed price vector \mathbf{x} , we define the uncertainty set \mathcal{U}^Γ as:

$$\mathcal{U}^\Gamma(\mathbf{x}) = \left\{ \tilde{\mathbf{g}}(\mathbf{x}) \in \mathbb{R}^n \mid \tilde{g}_i(x_i) = \hat{g}_i(x_i) + \xi_i \delta_i(x_i), \quad \sum_{i=1}^n |\xi_i| \leq \Gamma, \quad |\xi_i| \leq 1 \quad \forall i \right\}. \quad (12)$$

3.2 The Robust Counterpart

The robust margin constraint requires $S(\mathbf{x}) \geq 0$ for all $\tilde{\mathbf{g}} \in \mathcal{U}^\Gamma(\mathbf{x})$. Substituting the definitions of $N(\mathbf{x})$ and $D(\mathbf{x})$, this condition is equivalent to:

$$\min_{\tilde{\mathbf{g}} \in \mathcal{U}^\Gamma(\mathbf{x})} \sum_{i=1}^n \omega_i \tilde{g}_i(x_i) (x_i - \Delta a_i) \geq 0. \quad (13)$$

Let $s_i(x_i) = \omega_i (x_i - \Delta a_i) \hat{g}_i(x_i)$ and $t_i(x_i) := \omega_i (x_i - \Delta a_i) \delta_i(x_i)$. The robust constraint can be rewritten as:

$$\sum_{i=1}^n s_i(x_i) + \min_{\xi: \sum |\xi_i| \leq \Gamma, |\xi_i| \leq 1} \sum_{i=1}^n t_i(x_i) \xi_i \geq 0. \quad (14)$$

The minimization term represents the worst-case deviation permitted by the budget. Since the objective is linear in ξ_i , the minimum is achieved when ξ_i takes values on the boundary of its domain to oppose the sign of $\omega_i(x_i - \Delta a_i)$. This worst-case behavior leads to the following exact formulation:

Theorem 2 (Robust Counterpart Formulation). *Let $\Gamma \in \{0, 1, \dots, n\}$ be an integer. Define*

$$\beta(\mathbf{x}, \Gamma) := \sum_{k=1}^{\Gamma} |t|_{(k)}(\mathbf{x}),$$

where $|t|_{(1)}(\mathbf{x}) \geq \dots \geq |t|_{(n)}(\mathbf{x})$ denotes the nonincreasing ordering of the numbers $\{|t_i(x_i)|\}_{i=1}^n$. We adopt the convention that $\beta(\mathbf{x}, 0) = 0$. Then the robust optimization problem is equivalent to

$$\max_{\mathbf{x}} \sum_{i=1}^n \omega_i x_i \hat{g}_i(x_i) \quad (15)$$

$$s.t. \quad \sum_{i=1}^n s_i(x_i) - \beta(\mathbf{x}, \Gamma) \geq 0, \quad (16)$$

$$x_i \in [(1 - \sigma_i)a_i, (1 + \sigma_i)a_i] \cap \mathcal{X}_i \quad (\forall i).$$

Proof. Fix \mathbf{x} and consider the inner minimization in (14):

$$V(\mathbf{x}) = \min_{\substack{\sum_{i=1}^n |\xi_i| \leq \Gamma \\ |\xi_i| \leq 1}} \sum_{i=1}^n t_i(x_i) \xi_i.$$

By feasibility and symmetry of the constraints, for any feasible $\boldsymbol{\xi}$ we may flip signs coordinatewise so that $\text{sgn}(\xi_i) = -\text{sgn}(t_i(x_i))$ whenever $\xi_i \neq 0$, without violating $\sum_i |\xi_i| \leq \Gamma$ or $|\xi_i| \leq 1$. This is valid because $|\xi_i|$ is invariant under sign changes, so neither the budget constraint nor the box constraint is affected. Hence

$$V(\mathbf{x}) = - \max_{\substack{\sum_{i=1}^n y_i \leq \Gamma \\ 0 \leq y_i \leq 1}} \sum_{i=1}^n |t_i(x_i)| y_i, \quad \text{where } y_i := |\xi_i|.$$

The maximization problem above is a linear program. Since Γ is an integer, it admits an optimal extreme point solution with $y_i \in \{0, 1\}$ for all i and $\sum_i y_i \leq \Gamma$. Therefore an optimal solution sets $y_i = 1$ for the Γ indices with largest coefficients $|t_i(x_i)|$ and $y_i = 0$ otherwise, giving

$$V(\mathbf{x}) = - \sum_{k=1}^{\Gamma} |t|_{(k)}(\mathbf{x}) = -\beta(\mathbf{x}, \Gamma).$$

Substituting this into (14) yields (16). □

4 Structural Analysis and Greedy Optimality

The Γ -budget penalty $\beta(\mathbf{x}, \Gamma)$ couples items and breaks separability, which is a main source of computational difficulty in robust discrete pricing. Even without robustness, the reduced problem is NP-hard because it is an MCKP. The key structural observation is that the LP relaxation remains efficiently solvable: each item's discrete menu induces an upper hull in the cost-value plane, and the global LP reduces to greedy filling over hull segments. The sequel derives this hull-greedy LP structure and connects it to the robust model through the parametric decomposition used in [Section 5](#).

4.1 Upper-hull geometry of the LP relaxation

Fix an item i and consider its admissible discrete options $x_{i,j} \in \mathcal{X}_i^{\text{ad}}$ from [Section 1](#). Each option induces a point (c_{ij}, v_{ij}) in the cost–value plane, and we write

$$\mathcal{P}_i := \{(c_{ij}, v_{ij}) : x_{i,j} \in \mathcal{X}_i^{\text{ad}}\} \subset \mathbb{R}^2.$$

In the LP relaxation, the constraints $\sum_j z_{ij} = 1$ and $z_{ij} \geq 0$ allow fractional mixing across options; equivalently, item i may realize any aggregate point $(c_i, v_i) \in \text{conv}(\mathcal{P}_i)$. Since the objective maximizes value for a given resource usage, only points on the *upper hull* of $\text{conv}(\mathcal{P}_i)$ can be optimal. This motivates *upper-hull filtering*: we replace \mathcal{P}_i by the ordered vertex sequence \mathcal{H}_i of the upper hull of $\text{conv}(\mathcal{P}_i)$, thereby discarding dominated menu points without changing the LP optimum.

Remark 3. (Economic intuition) In many pricing portfolios, spending additional margin slack yields progressively smaller revenue gains, suggesting a concave “efficiency frontier”. The analysis below does not assume such concavity on the raw discrete menus: concavity arises automatically after passing to the upper hull of $\text{conv}(\mathcal{P}_i)$.

Assume the LP is feasible, equivalently $C \geq \sum_i \min_j c_{ij}$ (and in particular $C \geq \sum_i c_{i,1}^H$).

Remark 4 (Relation to prior work). The properties collected in [Theorem 5](#) are individually standard in the MCKP literature; see [Dyer \(1984\)](#), [Pisinger \(1995\)](#), and [Kellerer et al. \(2004, Chapter 11\)](#). We re-prove them in unified form because our notation differs from these sources and the segment parameterization is used directly in [Section 5](#). Readers familiar with the classical MCKP LP structure may skip ahead to the Robust Constraint Structure subsection without loss of continuity.

Theorem 5 (Hull reduction and greedy optimality for the LP relaxation). *Consider the LP relaxation of the Multiple-Choice Knapsack Problem (MCKP):*

$$\begin{aligned} \max_z \quad & \sum_{i=1}^n \sum_{j=1}^m v_{ij} z_{ij} \\ \text{s.t.} \quad & \sum_{i=1}^n \sum_{j=1}^m c_{ij} z_{ij} \leq C, \\ & \sum_{j=1}^m z_{ij} = 1 \quad (i = 1, \dots, n), \\ & z_{ij} \geq 0 \quad (\forall i, j). \end{aligned} \tag{17}$$

For each item i , define the point set $\mathcal{P}_i := \{(c_{ij}, v_{ij}) : j = 1, \dots, m\} \subset \mathbb{R}^2$. Let $\mathcal{H}_i = \{(c_{i,1}^H, v_{i,1}^H), \dots, (c_{i,p_i}^H, v_{i,p_i}^H)\}$ denote the vertices of the upper hull of $\text{conv}(\mathcal{P}_i)$, ordered so that $c_{i,1}^H < \dots < c_{i,p_i}^H$. For $k = 1, \dots, p_i - 1$ define the hull segment lengths and slopes

$$\Delta c_{i,k}^H := c_{i,k+1}^H - c_{i,k}^H > 0, \quad \rho_{i,k}^H := \frac{v_{i,k+1}^H - v_{i,k}^H}{c_{i,k+1}^H - c_{i,k}^H}.$$

Then the following statements hold.

- (i) (**Upper-hull sufficiency / two-adjacent-vertices mixing.**) *There exists an optimal solution to (17) such that for each i , the induced aggregate point $(c_i, v_i) := (\sum_j c_{ij} z_{ij}, \sum_j v_{ij} z_{ij})$ lies on the upper hull of $\text{conv}(\mathcal{P}_i)$, and hence can be represented as a convex combination of at most two adjacent hull vertices $(c_{i,k}^H, v_{i,k}^H)$ and $(c_{i,k+1}^H, v_{i,k+1}^H)$ for some k .*
- (ii) (**Reduction to continuous knapsack over hull segments.**) *The LP (17) is equivalent to the*

continuous knapsack problem

$$\begin{aligned}
\max_{\ell} \quad & \sum_{i=1}^n \sum_{k=1}^{p_i-1} \rho_{i,k}^H \ell_{i,k} \\
\text{s.t.} \quad & \sum_{i=1}^n \sum_{k=1}^{p_i-1} \ell_{i,k} \leq C - \sum_{i=1}^n c_{i,1}^H, \\
& 0 \leq \ell_{i,k} \leq \Delta c_{i,k}^H \quad (\forall i, k),
\end{aligned} \tag{18}$$

where $\ell_{i,k}$ denotes the amount of capacity allocated to hull segment k of item i .

(iii) (**Greedy optimality for the LP relaxation.**) Let ℓ^* be obtained by filling segment variables $\ell_{i,k}$ in nonincreasing order of densities $\rho_{i,k}^H$, each up to its upper bound $\Delta c_{i,k}^H$, with at most one final fractional fill to meet the capacity constraint. Then ℓ^* induces an optimal solution to (18) and hence an optimal solution to the LP relaxation (17). In particular, there exists an optimal LP solution in which at most one item is mixed fractionally (i.e. across two adjacent hull vertices); all other items select a single hull vertex.

(iv) (**Special case: incremental greedy on the raw chain.**) Suppose for every i the raw point chain $\{(c_{i,j}, v_{i,j})\}_{j=1}^m$ satisfies $c_{i,1} < \dots < c_{i,m}$ and lie on the upper hull of $\text{conv}(\mathcal{P}_i)$. Thus they coincide with the hull vertices. Then the greedy rule in (iii) reduces to the incremental greedy algorithm on adjacent increments $\rho_{i,j} = (v_{i,j} - v_{i,j-1}) / (c_{i,j} - c_{i,j-1})$.

Proof. Steps 1–3 (convex-hull reformulation, restriction to the upper hull, and segment-length parameterization) follow standard arguments adapted to our notation; we defer them to Section B for completeness.

Proof of (iii). Problem (18) is a continuous knapsack (fractional) problem with items indexed by pairs (i, k) , value density $\rho_{i,k}^H$ and capacity upper bound $\Delta c_{i,k}^H$. A standard exchange argument shows that an optimal solution is obtained by filling variables in nonincreasing order of $\rho_{i,k}^H$: take two variables (i, k) and (i', k') with $\rho_{i,k}^H > \rho_{i',k'}^H$. If $0 < \ell_{i',k'} < \Delta c_{i',k'}^H$ while $\ell_{i,k} < \Delta c_{i,k}^H$, then shifting an infinitesimal amount ε of capacity from $\ell_{i',k'}$ to $\ell_{i,k}$ increases the objective by $\varepsilon(\rho_{i,k}^H - \rho_{i',k'}^H) > 0$ while preserving feasibility, contradicting optimality. Thus, in any optimum, all higher-density variables are saturated before any lower-density variable is positive, implying the greedy fill rule is optimal and that at most one variable can be fractional at termination. This proves (iii).

Proof of (iv). If for each i the raw chain coincides with the hull vertices, i.e. $\mathcal{H}_i = \{(c_{i,j}, v_{i,j})\}_{j=1}^m$, then the hull segments are exactly the adjacent increments $(j-1) \rightarrow j$ and $\rho_{i,k}^H$ equals $\rho_{i,j}$. Therefore the greedy rule in (iii) reduces to selecting adjacent upgrades in descending order of $\rho_{i,j}$, which is precisely the incremental greedy algorithm. \square

4.2 Robust Constraint Structure

4.2.1 Box Uncertainty ($\Gamma = n$): Separability

We first address the structural impact of robustness in the limiting case of **Box Uncertainty**, i.e. when the budget equals the number of items ($\Gamma = n$). In this regime, every item may simultaneously deviate to its worst-case limit.

Recall the robust margin constraint in the form (14):

$$\sum_{i=1}^n s_i(x_i) + \min_{\substack{\sum_{i=1}^n |\xi_i| \leq \Gamma \\ |\xi_i| \leq 1}} \sum_{i=1}^n t_i(x_i) \xi_i \geq 0, \quad s_i(x) = \omega_i(x - \Delta a_i) \hat{g}_i(x), \quad t_i(x) = \omega_i(x - \Delta a_i) \delta_i(x).$$

For $\Gamma = n$, the budget constraint $\sum_i |\xi_i| \leq n$ is redundant given $|\xi_i| \leq 1$, and the inner minimum is attained by choosing $\xi_i = -\text{sgn}(t_i(x_i))$, yielding

$$\sum_{i=1}^n s_i(x_i) - \sum_{i=1}^n |t_i(x_i)| \geq 0. \quad (19)$$

Hence the box-robust pricing problem can be written as

$$\begin{aligned} \max_{\mathbf{x}} \quad & \sum_{i=1}^n v_i(x_i) \quad \text{where } v_i(x) := \omega_i x \hat{g}_i(x), \\ \text{s.t.} \quad & \sum_{i=1}^n \left(s_i(x_i) - |t_i(x_i)| \right) \geq 0, \\ & x_i \in X_i \cap [(1 - \sigma_i)a_i, (1 + \sigma_i)a_i] \quad (\forall i). \end{aligned} \quad (20)$$

In contrast to the coupled case $\Gamma < n$, the penalty in (19) is additive and therefore separable across items.

4.2.2 Coupled Uncertainty ($\Gamma < n$): Parametric Decomposition

For the coupled case $\Gamma < n$, items interact through the shared uncertainty budget. By [Theorem 2](#), the robust margin constraint is equivalent to

$$\sum_{i=1}^n s_i(x_i) - \beta(\mathbf{x}, \Gamma) \geq 0, \quad (21)$$

where $\beta(\mathbf{x}, \Gamma) = \sum_{k=1}^{\Gamma} |t|_{(k)}(\mathbf{x})$ is the sum of the Γ largest values of $\{|t_i(x_i)|\}_{i=1}^n$. While this characterization is explicit, direct optimization over $\beta(\mathbf{x}, \Gamma)$ is difficult because it couples all items through a sorting operation. We resolve this by observing that $\beta(\mathbf{x}, \Gamma)$ admits a dual scalar representation:

$$\beta(\mathbf{x}, \Gamma) = \max_{\xi} \left\{ \sum_{i=1}^n |t_i(x_i)| \xi_i \mid \sum_{i=1}^n \xi_i \leq \Gamma, 0 \leq \xi_i \leq 1 \forall i \right\}. \quad (22)$$

Theorem 6 (Parametric decomposition of the coupled Γ -budget penalty). *For every \mathbf{x} , the penalty $\beta(\mathbf{x}, \Gamma)$ in (22) admits the dual representation*

$$\beta(\mathbf{x}, \Gamma) = \min_{\theta \geq 0} \left\{ \Gamma\theta + \sum_{i=1}^n \max \{0, |t_i(x_i)| - \theta\} \right\}. \quad (23)$$

Consequently, the robust margin constraint (21) holds if and only if there exists $\theta \geq 0$ such that

$$\sum_{i=1}^n \left(s_i(x_i) - \max \{0, |t_i(x_i)| - \theta\} \right) \geq \Gamma\theta. \quad (24)$$

For any fixed $\theta \geq 0$, the left-hand side of (24) is separable across items.

Proof. Fix \mathbf{x} . Problem (22) is a feasible and bounded linear program over a nonempty compact polytope. Its dual is

$$\min_{\theta \geq 0, \pi \geq 0} \Gamma\theta + \sum_{i=1}^n \pi_i \quad \text{s.t.} \quad \theta + \pi_i \geq |t_i(x_i)| \quad (\forall i).$$

Strong duality yields equality of primal and dual optimal values. For any fixed $\theta \geq 0$, the minimal feasible choice is $\pi_i = \max\{0, |t_i(x_i)| - \theta\}$, which gives (23). Substituting (23) into (21) yields (24). \square

5 A Robust Hull-Greedy Algorithm for the Discrete Problem

We develop a method for the *discrete* Γ -budget robust pricing problem. After the reduction in [Section 1](#), the problem is an MCKP and remains NP-hard, so we target exact robust-feasibility certification together with explicit performance guarantees relative to LP benchmarks. The algorithm is driven by two structural results: the one-dimensional parametric reformulation of the coupled robust constraint ([Theorem 6](#)) and the exact hull-greedy solution of the fixed-parameter LP relaxation ([Theorem 5](#)).

5.1 Exact robust feasibility via a scalar parameter

For each admissible option $x_{i,j} \in \mathcal{X}_i^{\text{ad}}$, define

$$v_{ij} := \omega_i x_{i,j} \hat{g}_i(x_{i,j}), \quad s_{ij} := \omega_i (x_{i,j} - \Delta a_i) \hat{g}_i(x_{i,j}), \quad t_{ij} := \omega_i (x_{i,j} - \Delta a_i) \delta_i(x_{i,j}).$$

By [Theorem 6](#), the robust margin constraint is equivalent to the existence of $\theta \geq 0$ such that

$$\sum_{i=1}^n \left(s_i(x_i) - \max\{0, |t_i(x_i)| - \theta\} \right) \geq \Gamma \theta. \quad (25)$$

For fixed $\theta \geq 0$, introduce the per-option θ -modified contributions

$$s_{ij}^\theta := s_{ij} - \max\{0, |t_{ij}| - \theta\}. \quad (26)$$

Then (25) becomes the separable inequality

$$\sum_{i=1}^n s_{i,j(i)}^\theta \geq \Gamma \theta, \quad j(i) \in \{1, \dots, m\} \text{ chosen for each } i. \quad (27)$$

where $j(i)$ denotes the index of the option selected for item i .

Proposition 7 (Finite candidate set for θ). *Let*

$$\mathcal{B} := \{0\} \cup \{|t_{ij}| : i = 1, \dots, n, x_{i,j} \in \mathcal{X}_i^{\text{ad}}\}.$$

If the discrete robust problem is feasible, then there exists an optimal solution (\mathbf{x}^, θ^*) with $\theta^* \in \mathcal{B}$.*

Proof. Fix a discrete \mathbf{x} . Define

$$f_{\mathbf{x}}(\theta) := \sum_{i=1}^n \left(s_i(x_i) - \max\{0, |t_i(x_i)| - \theta\} \right) - \Gamma \theta.$$

Then $f_{\mathbf{x}}$ is concave piecewise-affine in θ , with breakpoints contained in $\{0\} \cup \{|t_i(x_i)|\}_{i=1}^n$. If $f_{\mathbf{x}}(\theta_0) \geq 0$ for some $\theta_0 \geq 0$, let $[\theta_L, \theta_U]$ be the maximal interval containing θ_0 on which $f_{\mathbf{x}}$ is affine (so θ_L, θ_U are breakpoints, with $\theta_L = \theta_U = \theta_0$ possible). Since $f_{\mathbf{x}}$ is affine on $[\theta_L, \theta_U]$, at least one endpoint satisfies $f_{\mathbf{x}}(\theta) \geq 0$ (because a non-negative affine function on an interval attains its minimum at an endpoint), and thus feasibility for fixed \mathbf{x} can always be certified by some breakpoint $\theta \in \{0\} \cup \{|t_i(x_i)|\}_{i=1}^n$. Because each $|t_i(x_i)|$ equals $|t_{i,j(i)}|$ for some admissible option, every such value belongs to \mathcal{B} . Since this argument holds for every discrete \mathbf{x} individually, the joint optimum (\mathbf{x}^*, θ^*) is covered by enumerating $\theta \in \mathcal{B}$ and, for each fixed θ , optimizing over discrete \mathbf{x} —which is precisely the structure exploited by [Algorithm 1](#). \square

5.2 Fixed- θ reformulation as an MCKP

Fix $\theta \in \mathcal{B}$. Convert (27) into a knapsack inequality with nonnegative costs via a baseline–slack transformation. For each item i , choose

$$j^\theta(i) \in \arg \max_j s_{ij}^\theta, \quad S_{\max}^\theta := \sum_{i=1}^n s_{i,j^\theta(i)}^\theta, \quad c_{ij}^\theta := s_{i,j^\theta(i)}^\theta - s_{ij}^\theta \ (\geq 0).$$

Then (27) is equivalent to

$$\sum_{i=1}^n c_{i,j^\theta(i)}^\theta \leq C^\theta, \quad C^\theta := S_{\max}^\theta - \Gamma\theta. \quad (28)$$

Thus, for fixed θ , robust-feasible discrete pricing is exactly the MCKP

$$\max \sum_{i=1}^n v_{i,j^\theta(i)} \quad \text{s.t.} \quad \sum_{i=1}^n c_{i,j^\theta(i)}^\theta \leq C^\theta, \quad x_{i,j^\theta(i)} \in \mathcal{X}_i^{\text{ad}} \ (\forall i). \quad (29)$$

5.3 Upper-hull filtering and an exact LP solver for fixed θ

Fix $\theta \in \mathcal{B}$ with $C^\theta \geq 0$. Item i induces the point set

$$\mathcal{P}_i^\theta := \{(c_{ij}^\theta, v_{ij}) : x_{i,j} \in \mathcal{X}_i^{\text{ad}}\} \subset \mathbb{R}^2.$$

Before computing the hull, apply a standard preprocessing step: (a) if multiple points share the same cost c , keep only the one with largest value v ; (b) remove dominated points (if $c \leq c'$ and $v \geq v'$, discard (c', v')). This does not change the upper hull. Apply *upper-hull filtering* by replacing \mathcal{P}_i^θ with the ordered vertex sequence

$$\mathcal{H}_i^\theta = \{(c_{i,1}^{H,\theta}, v_{i,1}^{H,\theta}), \dots, (c_{i,p_i}^{H,\theta}, v_{i,p_i}^{H,\theta})\}$$

of the upper hull of $\text{conv}(\mathcal{P}_i^\theta)$ (ordered by increasing c). Since \mathcal{H}_i^θ consists of vertices of $\text{conv}(\mathcal{P}_i^\theta)$, each hull vertex is one of the original menu points (c_{ij}^θ, v_{ij}) and therefore corresponds to a discrete option. Define hull segment lengths and slopes

$$\Delta c_{i,k}^{H,\theta} := c_{i,k+1}^{H,\theta} - c_{i,k}^{H,\theta} > 0, \quad \rho_{i,k}^{H,\theta} := \frac{v_{i,k+1}^{H,\theta} - v_{i,k}^{H,\theta}}{\Delta c_{i,k}^{H,\theta}} \quad (k = 1, \dots, p_i - 1).$$

By [Theorem 5](#), the LP relaxation of (29) is solved *exactly* by greedily filling hull segments in nonincreasing order of $\rho_{i,k}^{H,\theta}$. Moreover, there exists an optimal LP solution in which at most one item is fractional (mixed between two adjacent hull vertices).

Exact robust-feasibility certificate (final check). For any discrete price vector \mathbf{x} , robust feasibility can be certified directly by

$$\sum_{i=1}^n s_i(x_i) - \beta(\mathbf{x}, \Gamma) \geq 0, \quad \beta(\mathbf{x}, \Gamma) = \sum_{k=1}^{\Gamma} |t|_{(k)}(\mathbf{x}), \quad (30)$$

where $t_i(x) = \omega_i(x - \Delta a_i)\delta_i(x)$ and $|t|_{(1)}(\mathbf{x}) \geq \dots \geq |t|_{(n)}(\mathbf{x})$ are the sorted magnitudes.

5.4 Discrete recovery: one-item rounding with optional repair

Let $\mathbf{z}^{\text{LP}}(\theta)$ be an optimal LP solution produced by the hull-greedy procedure in [Section 5.3](#). If no item is fractional, it is already discrete. Otherwise, exactly one item i^* is mixed between two adjacent hull vertices $(c_{i^*,k}^{H,\theta}, v_{i^*,k}^{H,\theta})$ and $(c_{i^*,k+1}^{H,\theta}, v_{i^*,k+1}^{H,\theta})$.

Default choice (feasibility-preserving round-down). Rounding i^* down to the adjacent vertex with smaller knapsack cost c^θ weakly decreases total cost and thus preserves (28); all other items remain unchanged. This yields a feasible discrete solution $\mathbf{x}^\downarrow(\theta)$.

Optional improvement (round-up + repair). In practice, rounding down can lose a larger single-item value jump than necessary. As an optional refinement, also consider rounding i^* up to the higher vertex, obtaining $\mathbf{x}^\uparrow(\theta)$, which may violate (28) by some excess cost $\Delta C > 0$. If $\Delta C > 0$, restore feasibility by a *repair* step that performs discrete *downgrades* on other items along their hull chains: repeatedly select a downgrade that reduces knapsack cost by at least a small amount while minimizing loss of objective, specifically by selecting the downgrade $(i, k \rightarrow k-1)$ along item i 's hull chain that minimizes the ratio $(v_{i,k}^{H,\theta} - v_{i,k-1}^{H,\theta}) / (c_{i,k}^{H,\theta} - c_{i,k-1}^{H,\theta})$ among items with remaining downgrade capacity, until total cost is $\leq C^\theta$. Since downgrades weakly decrease total cost, feasibility is restored after finitely many steps. Finally, keep the better of the two feasible candidates,

$$\mathbf{x}(\theta) \in \arg \max \{N(\mathbf{x}^\downarrow(\theta)), N(\mathbf{x}^{\uparrow\text{-repair}}(\theta))\}.$$

This refinement is heuristic but feasibility-preserving. All theoretical guarantees (Propositions 8 and 9) apply to the round-down solution $\mathbf{x}^\downarrow(\theta)$ alone; the optional round-up-and-repair and completion steps can only improve the objective and are not required for the stated bounds.

Feasibility-preserving completion. While capacity remains, apply discrete *upgrades* along each item's hull chain (adjacent hull vertices) in decreasing order of slope among upgrades that fit. This can only improve the objective and preserves (28).

5.5 Complete algorithm and guarantees

We enumerate $\theta \in \mathcal{B}$ (which is sufficient by Proposition 7), solve the corresponding LP relaxation exactly by hull-greedy, and recover a discrete feasible solution by one-item rounding (optionally with repair/completion); see Algorithm 1.

Proposition 8 (Additive performance bound (per fixed θ)). *Fix $\theta \in \mathcal{B}$ with $C^\theta \geq 0$. Let $\text{OPT}_{\text{LP}}(\theta)$ and $\text{OPT}_{\text{IP}}(\theta)$ denote the optimal objective values of the LP relaxation of (29) and of (29), respectively. Let $\mathbf{x}(\theta)$ be the rounded solution produced by Algorithm 1 (before optional post-processing). Then*

$$\text{OPT}_{\text{LP}}(\theta) - N(\mathbf{x}(\theta)) \leq \Delta V_{\max}^\theta, \quad \text{and hence} \quad \text{OPT}_{\text{IP}}(\theta) - N(\mathbf{x}(\theta)) \leq \Delta V_{\max}^\theta,$$

where ΔV_{\max}^θ is defined in Section 5.6.

Proof. By Theorem 5(iii), there exists an optimal LP solution mixing at most one item between two adjacent hull vertices. Rounding down that item (to the adjacent vertex with smaller c^θ) preserves feasibility and decreases the objective by at most the corresponding adjacent value jump, bounded by ΔV_{\max}^θ . The second inequality follows from $\text{OPT}_{\text{LP}}(\theta) \geq \text{OPT}_{\text{IP}}(\theta)$. \square

Algorithm 1 Robust hull-greedy with θ -enumeration and discrete recovery

```

1: Input: admissible menus  $\{\mathcal{X}_i^{\text{ad}}\}$ , data  $(v_{ij}, s_{ij}, t_{ij})$ , budget  $\Gamma$ .
2: Form  $\mathcal{B} = \{0\} \cup \{|t_{ij}| : x_{i,j} \in \mathcal{X}_i^{\text{ad}}\}$ , deduplicate, and sort increasingly.
3:  $\text{BESTVAL} \leftarrow -\infty$ ,  $\text{BESTSOL} \leftarrow \emptyset$ .
4: for  $\theta \in \mathcal{B}$  do
5:   Compute  $s_{ij}^\theta$  via (26).
6:   Choose  $j^\theta(i) \in \arg \max_j s_{ij}^\theta$  and set  $c_{ij}^\theta = s_{i,j^\theta(i)}^\theta - s_{ij}^\theta$ .
7:    $C^\theta \leftarrow \sum_{i=1}^n s_{i,j^\theta(i)}^\theta - \Gamma\theta$ .
8:   if  $C^\theta < 0$  then continue.
9:   end if
10:  for  $i = 1, \dots, n$  do
11:    Build  $\mathcal{P}_i^\theta = \{(c_{ij}^\theta, v_{ij})\}_j$ .
12:    Preprocess  $\mathcal{P}_i^\theta$ : merge equal costs (keep max  $v$ ), then remove dominated points.
13:    Compute the upper hull  $\mathcal{H}_i^\theta$  and the slopes  $\rho_{i,k}^{H,\theta}$  and lengths  $\Delta c_{i,k}^{H,\theta}$ .
14:  end for
15:  Solve the LP relaxation of (29) exactly via hull-greedy over  $\rho_{i,k}^{H,\theta}$ .
16:  Recover a discrete solution  $\mathbf{x}(\theta)$  via Section 5.4 (round-down; optionally round-up+repair; optionally complete).
17:  Compute  $N(\mathbf{x}(\theta)) = \sum_{i=1}^n \omega_i x_i(\theta) \hat{g}_i(x_i(\theta))$ .
18:  Compute the exact robust certificate  $Z(\mathbf{x}(\theta)) := \sum_i s_i(x_i(\theta)) - \beta(\mathbf{x}(\theta), \Gamma)$  as in (30).
19:  if  $Z(\mathbf{x}(\theta)) < 0$  then continue.
20:  end if
21:  if  $N(\mathbf{x}(\theta)) > \text{BESTVAL}$  then
22:     $\text{BESTVAL} \leftarrow N(\mathbf{x}(\theta))$ ;  $\text{BESTSOL} \leftarrow (\theta, \mathbf{x}(\theta))$ .
23:  end if
24: end for
25: if  $\text{BESTSOL} = \emptyset$  then
26:   Output: INFEASIBLE (no  $\theta \in \mathcal{B}$  yields  $C^\theta \geq 0$  and a feasible selection).
27: else
28:   Output: BESTSOL.
29: end if

```

Practical note on θ enumeration. The set \mathcal{B} can be as large as $|\mathcal{B}| \leq nm + 1$, but in practice the search can be reduced substantially by restricting candidates to breakpoints induced by undominated options (after preprocessing). Moreover, (26) implies

$$s_{ij}^\theta = \begin{cases} s_{ij}, & \theta \geq |t_{ij}|, \\ s_{ij} - |t_{ij}| + \theta, & \theta < |t_{ij}|, \end{cases}$$

so s_{ij}^θ is piecewise-affine in θ with breakpoints at $|t_{ij}|$. Consequently, per-item maximizers $j^\theta(i) \in \arg \max_j s_{ij}^\theta$ can only change at such breakpoints, suggesting sweep-style implementations that update per-item baselines incrementally rather than recomputing from scratch. Regardless of the search strategy, the certificate (30) provides an exact final check.

5.6 Integrality gap and its asymptotic irrelevance

For benchmarking, we compare discrete solutions against the LP relaxation of (29). For fixed θ , $\text{OPT}_{\text{LP}}(\theta) \geq \text{OPT}_{\text{IP}}(\theta)$, and the gap is controlled by a *single* item.

Setup (fixed θ). Fix $\theta \in \mathcal{B}$ with $C^\theta \geq 0$. For each item i , let

$$\mathcal{P}_i^\theta := \{(c_{ij}^\theta, v_{ij}) : x_{i,j} \in \mathcal{X}_i^{\text{ad}}\} \subset \mathbb{R}^2,$$

and let $\mathcal{H}_i^\theta = \{(c_{i,1}^{H,\theta}, v_{i,1}^{H,\theta}), \dots, (c_{i,p_i}^{H,\theta}, v_{i,p_i}^{H,\theta})\}$ be the upper-hull vertex sequence of $\text{conv}(\mathcal{P}_i^\theta)$, ordered by strictly increasing cost $c_{i,1}^{H,\theta} < \dots < c_{i,p_i}^{H,\theta}$. Define the maximal adjacent hull jump

$$\Delta V_{\max}^\theta := \max_i \max_{k=1, \dots, p_i-1} (v_{i,k+1}^{H,\theta} - v_{i,k}^{H,\theta}) \geq 0,$$

with the convention $\max_{k \in \emptyset} (\cdot) = 0$ when $p_i = 1$.

Proposition 9 (Additive integrality-gap bound). *For every fixed $\theta \in \mathcal{B}$ with $C^\theta \geq 0$,*

$$0 \leq \text{OPT}_{\text{LP}}(\theta) - \text{OPT}_{\text{IP}}(\theta) \leq \Delta V_{\max}^\theta.$$

Proof. The lower bound is immediate since the LP relaxation enlarges the feasible set. For the upper bound, by [Theorem 5](#)(i)–(iii) there exists an optimal LP solution in which at most one item i^\star is fractional, and if fractional it mixes between two *adjacent* hull vertices $(c_{i^\star, k}^{H, \theta}, v_{i^\star, k}^{H, \theta})$ and $(c_{i^\star, k+1}^{H, \theta}, v_{i^\star, k+1}^{H, \theta})$ for some k . If no item is fractional, the LP solution is integral and the gap is 0.

Otherwise, the fractional point has the form

$$(c_{i^\star}, v_{i^\star}) = (1 - \alpha)(c_{i^\star, k}^{H, \theta}, v_{i^\star, k}^{H, \theta}) + \alpha(c_{i^\star, k+1}^{H, \theta}, v_{i^\star, k+1}^{H, \theta}), \quad \alpha \in (0, 1).$$

Round i^\star down to the cheaper endpoint $(c_{i^\star, k}^{H, \theta}, v_{i^\star, k}^{H, \theta})$ and keep all other items unchanged. Total knapsack cost weakly decreases, hence feasibility is preserved. The objective decreases by at most the adjacent jump $v_{i^\star, k+1}^{H, \theta} - v_{i^\star, k}^{H, \theta}$, because v_{i^\star} lies between the endpoint values. Thus

$$\text{OPT}_{\text{LP}}(\theta) - \text{OPT}_{\text{IP}}(\theta) \leq v_{i^\star, k+1}^{H, \theta} - v_{i^\star, k}^{H, \theta} \leq \Delta V_{\max}^\theta,$$

as claimed. □

Corollary 10 (Relative gap decays as $O(1/n)$). *Assume there exist constants $\bar{V} < \infty$ and $c > 0$ such that for all $\theta \in \mathcal{B}$,*

$$\Delta V_{\max}^\theta \leq \bar{V}, \quad \text{OPT}_{\text{LP}}(\theta) \geq c n.$$

Then for all $\theta \in \mathcal{B}$,

$$0 \leq \frac{\text{OPT}_{\text{LP}}(\theta) - \text{OPT}_{\text{IP}}(\theta)}{\text{OPT}_{\text{LP}}(\theta)} \leq \frac{\bar{V}}{c n} = O\left(\frac{1}{n}\right).$$

Proof. By [Proposition 9](#), $\text{OPT}_{\text{LP}}(\theta) - \text{OPT}_{\text{IP}}(\theta) \leq \Delta V_{\max}^\theta \leq \bar{V}$. Divide by $\text{OPT}_{\text{LP}}(\theta) \geq c n > 0$. □

When do \bar{V} and c exist? (Sufficient conditions) The assumptions $\Delta V_{\max}^\theta \leq \bar{V}$ and $\text{OPT}_{\text{LP}}(\theta) \geq c n$ express two standard regularities: (i) per-item value scales do not blow up, and (ii) the portfolio has nondegenerate average value. A convenient sufficient set is:

(A) Uniform bounded values. If there exists $M_v < \infty$ such that $0 \leq v_{ij} \leq M_v$ for all items i , all admissible options $j \in J_i^{\text{ad}}$, and all $\theta \in \mathcal{B}$, then $\Delta V_{\max}^\theta \leq M_v$ for all θ (take $\bar{V} := M_v$), since hull vertices are menu points and differences of two numbers in $[0, M_v]$ are at most M_v . A concrete sufficient condition for such an M_v is $\sup_i \omega_i < \infty$, $\sup_{i,j} x_{i,j} < \infty$, and $\sup_{i,j} \hat{g}_i(x_{i,j}) < \infty$, because then $v_{ij} = \omega_i x_{i,j} \hat{g}_i(x_{i,j})$ is uniformly bounded.

(B) Uniform positive value in a feasible baseline. If there exists $m_v > 0$ such that for each item i there is an admissible option $j \in J_i^{\text{ad}}$ that is feasible for the fixed- θ knapsack constraint and satisfies $v_{ij} \geq m_v$ (independently of n), then there is a feasible integer solution with value at least $m_v n$, hence $\text{OPT}_{\text{LP}}(\theta) \geq \text{OPT}_{\text{IP}}(\theta) \geq m_v n$ (take $c := m_v$). In pricing applications this is typically ensured by assuming each item has a “safe” admissible baseline price that preserves the margin constraint with slack, and exposures/demand at that baseline are bounded away from zero.

Practical implication. Under (A)–(B), the absolute LP–IP gap is controlled by a single-item jump while $\text{OPT}_{\text{LP}}(\theta) = \Omega(n)$, so the relative gap vanishes as $n \rightarrow \infty$. Hence the LP relaxation provides an essentially tight benchmark for large portfolios.

6 Numerical Results

We empirically examine three consequences of the structural analysis developed in Sections 4 and 5: (i) the rounding loss is bounded by a single hull jump and the relative gap decays as $O(1/n)$ (Proposition 9 and Corollary 10); (ii) the algorithm scales tractably, upper-hull filtering compresses per-item menus significantly, and the θ -enumeration is efficient in practice (Theorem 5 and Proposition 7); (iii) Γ -budget protection traces an interpretable revenue–risk frontier on the tested instances, consistent with the guarantee in Theorem 2.

6.1 Experimental protocol

Instance generator. We generate economically structured discrete pricing instances rather than uncorrelated knapsack data. For each item $i = 1, \dots, n$, we independently sample

$$a_i \sim \exp(\mathcal{N}(\mu=5, \tau^2=0.25)), \quad \omega_i \sim \exp(\mathcal{N}(\mu=0, \tau^2=0.09)),$$

Here $\mathcal{N}(\mu, \tau^2)$ denotes a normal distribution with mean μ and variance τ^2 ; the parameter τ is unrelated to the fairness tolerance σ_i in constraint (3). This yields reference prices with median ≈ 148 and exposures with median ≈ 1 , inducing realistic heterogeneity across the portfolio. We form a discrete menu of size m per item as $x_{i,j} = a_i(1 + u_{i,j})$ with $u_{i,j} \stackrel{\text{iid}}{\sim} \text{Uniform}(-0.15, 0.15)$ and restrict to the admissible set $\mathcal{X}_i^{\text{ad}} = \mathcal{X}_i \cap [(1 - \sigma_i)a_i, (1 + \sigma_i)a_i]$ with $\sigma_i = 0.10$ for all i . Nominal demand is monotone decreasing and piecewise linear:

$$\hat{g}_i(x) = b_i \max(0, 1 - \eta_i(x - a_i)/a_i), \quad b_i \sim \exp(\mathcal{N}(\mu=3, \tau^2=0.16)), \quad \eta_i \sim \text{Uniform}(1.5, 3.5),$$

(Note: This formulation intentionally allows demand to exceed the baseline without an upper bound as prices drop below the reference level.) with b_i and η_i sampled independently per item. Demand uncertainty is proportional to nominal demand, $\delta_i(x) = \alpha \hat{g}_i(x)$ with $\alpha \in \{0.10, 0.20\}$, which ensures $\delta_i(x) \leq \hat{g}_i(x)$ on $\mathcal{X}_i^{\text{ad}}$.

Nested (telescoping) instance design. To isolate the effect of portfolio size from cross-instance variation, we adopt a deterministic nested design throughout all experiments. We generate a single master portfolio of $n_{\text{max}} = 500$ items using a fixed seed (master seed 42 via `numpy.random.SeedSequence`), and evaluate *nested prefixes*: for each target size n , the instance consists of items $1, \dots, n$ from the master portfolio. This ensures that every item present at size n is also present at all sizes $n' > n$, so the *only* source of variation across the n -axis is the number of items. No replicates are needed; each (n, Γ) configuration corresponds to a single deterministic instance.

Margin-target calibration. We recalibrate Δ at each prefix size n so that the capacity slack remains controlled. Let \tilde{x}_i denote the admissible menu point closest to a_i ; then

$$\Delta(n) = (1 - \epsilon) \frac{\sum_{i=1}^n \omega_i \tilde{x}_i \hat{g}_i(\tilde{x}_i)}{\sum_{i=1}^n \omega_i a_i \hat{g}_i(\tilde{x}_i)}, \quad \epsilon = 0.02,$$

so that the baseline policy retains a relative slack of 2% regardless of the absolute scale of the margin ratio. This ensures that the knapsack capacity after the baseline–slack transformation is tight enough to make upgrades nontrivial across all portfolio sizes.

Scaling regime. Unless stated otherwise we use $m = 50$ and portfolio sizes $n \in \{30, 50, 75, 100, 150, 200, 300, 500\}$. Robustness budgets are $\Gamma \in \{0, \lfloor \sqrt{n} \rfloor, \lfloor 0.1n \rfloor\}$ unless otherwise varied. Wall-clock times are measured on a single thread, excluding I/O and plotting.

Implementation details. All experiments were implemented in Python 3.14. Runtime (“time”) refers to wall-clock seconds measured on a single thread on an Apple M4, 16 GB RAM, running macOS 26.3.1.

Benchmarks. For each candidate $\theta \in \mathcal{B}$ evaluated by Algorithm 1, the LP relaxation value $\text{OPT}_{\text{LP}}(\theta)$ returned by hull-greedy serves as the primary benchmark. For $n \leq 200$ we additionally solve the fixed- θ discrete MCKP as a MILP (HiGHS, time limit 120 s) at the θ selected by Algorithm 1 to obtain $\text{OPT}_{\text{IP}}(\theta)$. For $n \leq 75$ we additionally perform a *global* discrete benchmark: we enumerate all $\theta \in \mathcal{B}$, solve the MILP at each (time limit 600 s), and take the best objective across all θ , yielding a true global discrete optimum against which our θ -selection can be validated. All numerical results reported in Sections 6.2–6.5 use the full pipeline of Algorithm 1: round-down, followed by the optional round-up-with-repair step, followed by feasibility-preserving completion (Section 5.4). The rounding loss L_{rd} reported below, however, is always measured relative to the round-down solution $\mathbf{x}^\downarrow(\theta)$ before repair and completion, so that it directly tests the theoretical bound of Proposition 9. The final objective $N(\mathbf{x}(\theta))$ used for revenue comparisons and Table 1 is the post-repair value, which is weakly better. Solution quality is measured by the absolute rounding loss

$$L_{\text{rd}}(\theta) := \text{OPT}_{\text{LP}}(\theta) - N(\mathbf{x}^\downarrow(\theta)),$$

which is the quantity directly bounded by $\Delta V_{\text{max}}^\theta$ in Proposition 9, and by the relative gap $\text{Gap}_{\text{LP}}(\theta) := L_{\text{rd}}(\theta)/\text{OPT}_{\text{LP}}(\theta)$. Robust feasibility is certified by (30).

LP solver validation. As a prerequisite check, we cross-validated the hull-greedy LP solver against HiGHS (via `scipy.optimize.linprog`) on all prefix instances, at the algorithm’s optimal θ as well as at $\theta = 0$ and $\theta = \max \mathcal{B}$. In all cases the absolute objective residual satisfies $|r| < 10^{-8}$, the greedy critical slope agrees with the HiGHS dual variable on the knapsack constraint to the same precision, and the hull-greedy LP solution has at most one fractional item, consistent with Theorem 5. These results are not shown separately, as they serve as a correctness check rather than a standalone finding.

6.2 Integrality gap and $O(1/n)$ decay

We validate the additive bound of Proposition 9 ($L_{\text{rd}} \leq \Delta V_{\text{max}}^\theta$) and the consequent relative-gap decay of Corollary 10 ($\text{Gap}_{\text{LP}} = O(1/n)$).

Setup. Fix $m = 50$, $\alpha = 0.10$, and evaluate nested prefixes at $n \in \{30, 50, 75, 100, 150, 200, 300, 500\}$ for each of the three Γ -regimes. For each (n, Γ) pair we record the absolute rounding loss L_{rd} (from the round-down step alone), the theoretical bound $\Delta V_{\text{max}}^\theta$ (the maximal adjacent value jump on the upper hull at the algorithm’s optimal θ), and the LP objective $\text{OPT}_{\text{LP}}(\theta)$.

Choice of metric. The core theoretical prediction is the additive bound $L_{\text{rd}} \leq \Delta V_{\text{max}}^\theta$ (Proposition 9). Since $\Delta V_{\text{max}}^\theta$ is a single-item quantity and $\text{OPT}_{\text{LP}}(\theta) = \Omega(n)$, the relative gap $\text{Gap}_{\text{LP}} = L_{\text{rd}}/\text{OPT}_{\text{LP}} = O(1/n)$ follows as a direct consequence (Corollary 10). We plot the *ratio* $L_{\text{rd}}/\Delta V_{\text{max}}^\theta$ to test the additive bound (the prediction is simply that the ratio lies below 1), and the *scaled gap* $n \times \text{Gap}_{\text{LP}}$ to test the $O(1/n)$ rate (the prediction is that this quantity remains bounded as n grows). Both metrics avoid the numerical-floor artifact that arises when plotting $\text{Gap}_{\text{LP}} \sim 10^{-8}$ directly.

Additive bound. Figure 1a displays the normalized rounding loss $L_{\text{rd}}/\Delta V_{\text{max}}^\theta$ as a function of n for the three Γ -regimes. All 24 data points lie well below the dashed threshold at 1, consistent with the additive bound of Proposition 9. The maximum observed ratio is 0.31 (at $n = 30$, $\Gamma = \lfloor 0.1n \rfloor = 3$); for $n \geq 100$ the ratio stays below 0.15 across all regimes, indicating that the bound carries substantial slack in practice.

$O(1/n)$ **decay.** Figure 1b plots the scaled gap $n \times \text{Gap}_{\text{LP}}$ against n . If $\text{Gap}_{\text{LP}} = O(1/n)$ then this product should remain bounded; if the rate were faster than $O(1/n)$ the product would trend downward, and if slower it would diverge. The data fluctuate around a stable median of approximately 0.007 (dashed line) with no systematic trend, consistent with the predicted $O(1/n)$ rate across all three Γ -regimes. Point-to-point variation (e.g. the spike at $n = 300$ for $\Gamma = 0$) reflects changes in the identity of the fractional item as the prefix grows—an inherent feature of the deterministic nested design, not estimation noise.

MILP and global benchmarks. Where MILP results are available ($n \leq 200$), the discrete optimum $\text{OPT}_{\text{IP}}(\theta)$ agrees with our rounded solution to within 0.01% at the same θ , indicating that the rounding loss is negligible relative to the LP–IP gap. For $n \leq 75$, the global discrete benchmark (best MILP across all θ) agrees with the Algorithm 1 objective to within 0.01%, indicating that the θ -selection is near-optimal.

Consistency with the sufficient conditions in Corollary 10. The $O(1/n)$ relative-gap decay of Corollary 10 requires two regularity conditions: (A) a uniform bound $\Delta V_{\text{max}}^\theta \leq \bar{V}$ and (B) a linear lower bound $\text{OPT}_{\text{LP}}(\theta) \geq c n$. On the deterministic nested-prefix test bed generated in Section 6.1, both conditions hold instance-wise for elementary finite-sample reasons. For (A), all tested prefixes are drawn from a single finite master instance, so the realized value coefficients and hence the realized adjacent hull jumps form a finite set, which admits a common finite upper bound. For (B), whenever $C^\theta \geq 0$, the fixed- θ formulation admits the zero-cost baseline choice $j^\theta(i) \in \arg \max_j s_{ij}^\theta$ for each item, yielding a feasible LP solution with objective at least $\sum_{i=1}^n v_{i,j^\theta(i)}$; since all realized admissible menu values are strictly positive in the generated instance, this gives a linear lower bound of the form $m_\nu n$ for some realized constant $m_\nu > 0$. Accordingly, the empirical $O(1/n)$ decay observed in Figure 1b is consistent with the theoretical prediction on this test bed.

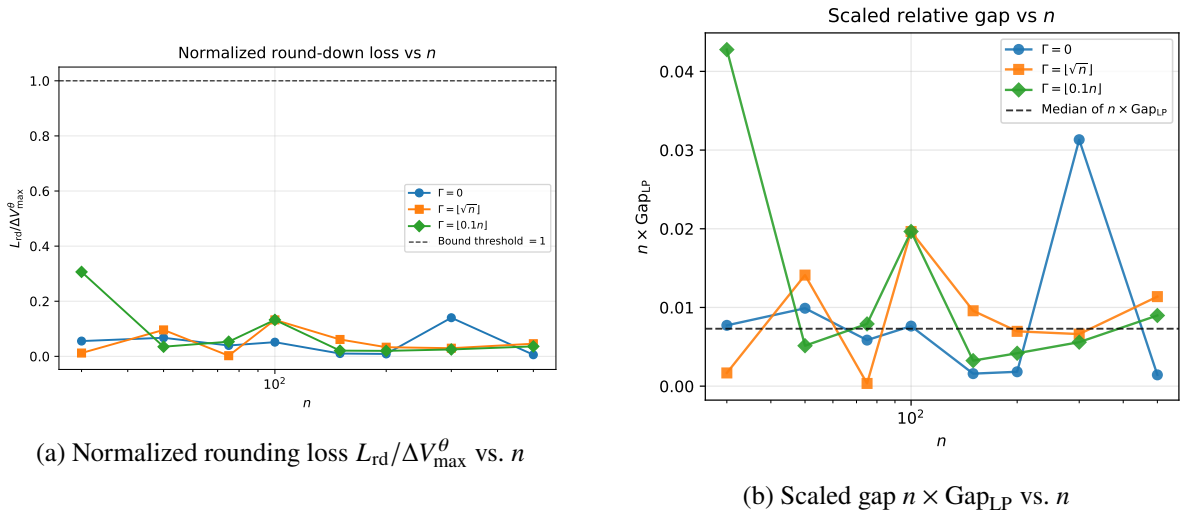


Figure 1: Integrality gap (Proposition 9 and Corollary 10). (a) Ratio of round-down loss to additive bound vs. n for three Γ -regimes; all points lie well below the theoretical ceiling of 1 (dashed), consistent with Proposition 9. (b) Scaled relative gap $n \times \text{Gap}_{\text{LP}}$ vs. n ; the product fluctuates around a stable median (dashed) with no upward trend, consistent with the $O(1/n)$ decay of Corollary 10.

6.3 Scalability, hull compression, and θ -enumeration efficiency

We assess the practical scalability of Algorithm 1, the compression achieved by upper-hull filtering (Theorem 5(i)–(ii)), and the efficiency of the θ -enumeration (Proposition 7).

Runtime scaling. Fix $\alpha = 0.10$, $\Gamma = \lfloor \sqrt{n} \rfloor$, and consider

$$m \in \{10, 50\}, \quad n \in \{30, 50, 75, 100, 150, 200, 300, 500\}.$$

We record total wall-clock time and a per-phase breakdown (preprocessing, θ -loop overhead, hull computation, greedy filling, rounding, and certification).

Figure 2a shows total runtime on log-log axes with separate curves per m . Both curves closely track the slope-2 reference line, indicating empirical scaling of approximately $O(n^2m)$ —consistent with $|\mathcal{B}| = O(nm)$ candidates each requiring $O(n)$ work for hull construction and greedy filling. The $m = 50$ curve sits roughly one order of magnitude above the $m = 10$ curve at every n , reflecting the linear dependence on menu size. At $n = 500$ and $m = 50$, the total runtime is approximately 400 s; for $m = 10$ the same portfolio size completes in roughly 30 s.

Figure 2c presents the runtime breakdown at $m = 50$ as a stacked bar chart. Hull construction (red) is overwhelmingly the dominant phase, accounting for the vast majority of wall-clock time at every n . All other phases—preprocessing, θ -loop overhead, greedy LP filling, rounding, and certification—are negligible by comparison. This indicates that hull construction is the computational bottleneck and that the sweep-style optimizations described in Section 5 (restricting \mathcal{B} to undominated breakpoints and caching hulls for unchanged items) target the dominant phase.

Hull compression. Since hull structure is a per-item property that is essentially independent of portfolio size n , we evaluate hull compression on the $n = 500$ master instance at $\theta = 0$ for $m \in \{10, 20, 50, 100\}$; this requires only a single hull construction per item (no θ -enumeration) and is computationally negligible.

Figure 2b shows the distribution of per-item hull sizes grouped by raw menu size m , with median values annotated. The median hull sizes are 7, 13, 33, and 67 for $m = 10, 20, 50$, and 100 respectively, corresponding to a compression ratio of roughly two-thirds across all menu sizes. Dashed reference lines at the raw m values show the gap between the full menu and the hull. While the compression ratio is approximately constant in m , the *absolute* reduction grows with menu size: at $m = 100$ the hull discards a median of 33 options per item, directly reducing the size of the candidate set \mathcal{B} and the per- θ hull construction cost.

θ -enumeration efficiency. For each instance we record $|\mathcal{B}|$ (after deduplication), the number of candidates skipped due to $C^\theta < 0$, and the number of distinct θ -values at which the final discrete objective $N(\mathbf{x}(\theta))$ strictly improves over the previous best. In all configurations, a large fraction of candidates is skipped early ($C^\theta < 0$), and among the evaluated candidates only a small subset improves the incumbent objective. The skip rate increases with portfolio size, consistent with the prediction of Proposition 7. Combined with the hull compression above, these two mechanisms—candidate reduction and early termination—help explain why the observed runtime appears close to quadratic in n for a fixed menu size m on the tested instances, rather than reflecting the most pessimistic worst-case bound.

Box-case cross-check ($\Gamma = n$). As an additional structural validation, we verify that for $\Gamma = n$ (box uncertainty) the general θ -enumeration algorithm produces the same solution as directly solving the separable formulation (20). On all tested prefix sizes the objectives match to machine precision, validating both the theory of Section 4 and the implementation.

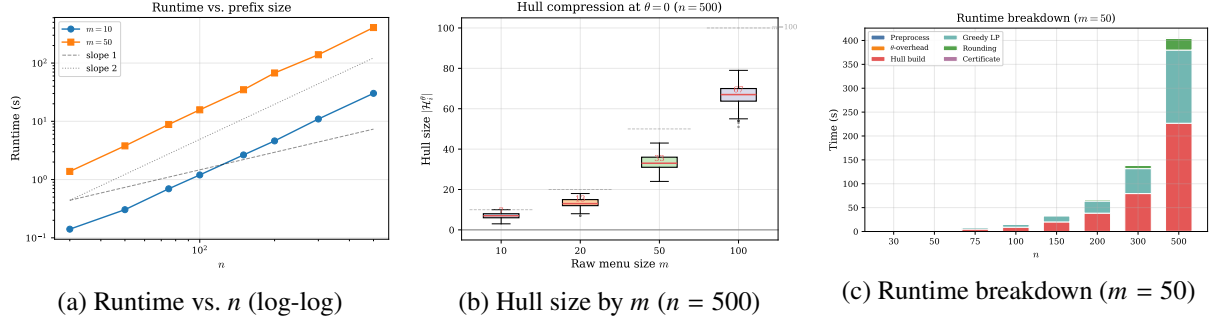


Figure 2: Scalability and hull compression. (a) Wall-clock runtime of Algorithm 1 vs. n for $m \in \{10, 50\}$; reference lines at slopes 1 and 2 are overlaid. Both curves track close to slope 2. (b) Box plot of per-item hull size $|\mathcal{H}_i^\theta|$ at $\theta = 0$, grouped by raw menu size m , on the $n = 500$ master instance; annotated values are medians. Dashed lines mark the raw menu size for reference; the hull retains roughly two-thirds of the menu across all m . (c) Stacked bar chart of runtime by algorithm phase ($m = 50$); hull construction dominates at every n .

6.4 Revenue–risk frontier

We quantify the practical value of Γ -budget protection (Theorem 2) and investigate the tightness of the guarantee.

Frontier construction. Fix $n = 200$ (the 200-item prefix of the master portfolio), $m = 50$, $\alpha \in \{0.10, 0.20\}$, and vary Γ over

$$\{0, 1, 3, 5, 10, \lfloor \sqrt{n} \rfloor, 20, 30, 50, 100, n\}.$$

For each solution \mathbf{x} we run $S = 10\,000$ Monte Carlo stress scenarios under two complementary perturbation protocols.

The first is an **adversarial (worst-case-direction)** stress test: by Theorem 2, the margin constraint can only be violated when deviations oppose the sign of $t_i(x_i)$. We sample $K \subset \{1, \dots, n\}$ with $|K| = \Gamma_{\text{attack}}$ uniformly at random, draw $\xi_i \sim \text{Uniform}(-1, 0)$ for $i \in K$, and set $\xi'_i := \xi_i \cdot \text{sgn}(t_i(x_i))$ so that each deviation opposes the margin contribution; for $i \notin K$, $\xi'_i := 0$. The attack level for the frontier plots is $\Gamma_{\text{attack}} = \max(\Gamma, \lfloor 1.5\Gamma \rfloor)$, which lies strictly above the protection budget for $\Gamma > 0$ and thus falls outside the certified uncertainty set \mathcal{U}^Γ .

The second is an **i.i.d. (stochastic)** stress test that models undirected demand noise: for every item i , independently draw $\xi_i \sim \text{Uniform}(-1, 1)$. In both cases, realized demand is $\tilde{g}_i(x_i) = \max(0, \hat{g}_i(x_i) + \xi'_i \delta_i(x_i))$ and the realized margin is $S_{\text{realized}} = \sum_i \omega_i(x_i - \Delta a_i) \tilde{g}_i$. We report violation probability $\hat{P} := S^{-1} \sum_{s=1}^S \mathbb{I}[S_{\text{realized}}^{(s)} < 0]$ and the 5%-quantile of S_{realized} .

Sanity check: zero observed violations at matching attack level. By construction, Theorem 2 guarantees $S(\mathbf{x}) \geq 0$ for all realizations in \mathcal{U}^Γ . Adversarial scenarios with $\Gamma_{\text{attack}} = \Gamma$ lie within \mathcal{U}^Γ and should produce zero observed violations. We observe this on all 22 configurations, providing a correctness check of both the certificate and the simulation.

Tightness of protection. To assess how tight the guarantee is, we additionally stress-test each Γ -protected solution at attack levels $\Gamma_{\text{attack}} \in \{\Gamma, \Gamma + \lfloor 0.1n \rfloor, 2\Gamma, n\}$. This shows that violations reappear once the attack exceeds the protection budget, directly illustrating the “price of robustness” interpretation of Bertsimas and Sim (2004).

Results. Figure 3a displays the revenue–risk frontier for $n = 200$ as two vertically aligned panels sharing a common Γ/n axis. The top panel shows normalized revenue: the cost of robustness is remarkably

small, with even full box protection ($\Gamma = n$) sacrificing less than 1% of nominal revenue in the synthetic frontier experiment for both $\alpha = 0.10$ and $\alpha = 0.20$. The revenue curve is smooth and concave, indicating diminishing marginal cost of additional protection. The bottom panel shows violation probability under both adversarial (solid) and i.i.d. (dashed) shocks at attack level $\Gamma_{\text{attack}} = \max(\Gamma, \lfloor 1.5\Gamma \rfloor)$. The nominal solution ($\Gamma = 0$) is highly vulnerable: adversarial violations reach approximately 50% and even undirected i.i.d. shocks produce violations roughly 30% of the time. Violations drop sharply to zero by $\Gamma/n \approx 0.05$ (i.e. $\Gamma \approx 10$), indicating that a modest protection budget covering 5% of the portfolio is sufficient to eliminate all observed violations under both perturbation protocols.

Figure 3b shows that the 5%-quantile of realized margin increases monotonically with Γ , with a concave profile: the steepest gains occur at small Γ/n , after which the curve flattens as additional protection yields diminishing tail-risk improvement. The $\alpha = 0.20$ curve lies above $\alpha = 0.10$ at every Γ because larger uncertainty amplitude induces the robust algorithm to build a larger margin buffer, resulting in a higher tail quantile under the adversarial stress test.

Figure 3c presents the tightness heatmap for $\alpha = 0.10$: rows index the protection level Γ , columns index Γ_{attack} , and color encodes violation probability on a logarithmic scale. Below and on the diagonal (dashed line at $\Gamma_{\text{attack}} = \Gamma$) the heatmap is white, indicating zero observed violations in line with Theorem 2. Above the diagonal, violation probability increases smoothly with the gap between attack and protection levels, exhibiting the staircase structure predicted by the Γ -budget model: each additional unit of protection shifts the white region one step further from the diagonal.

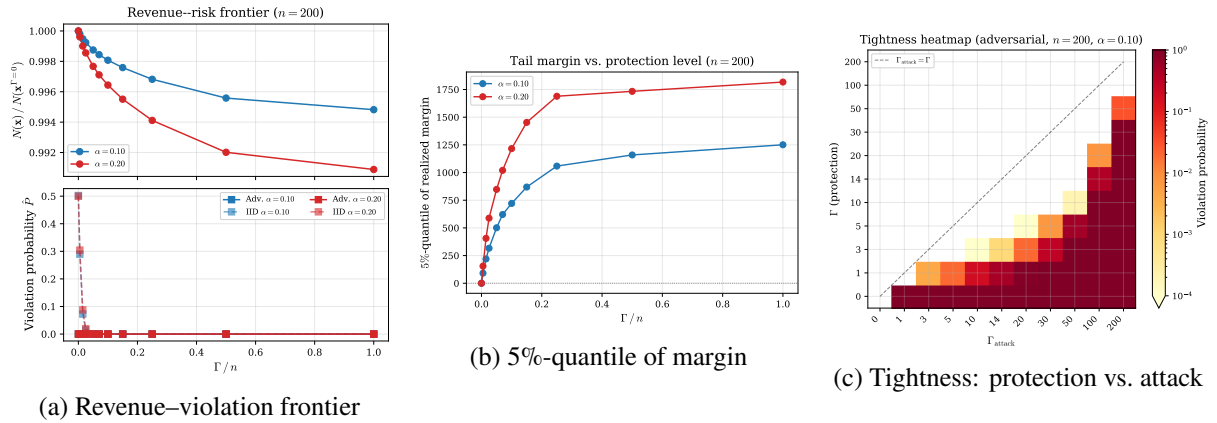


Figure 3: Revenue–risk frontier (Theorem 2, $n = 200$). (a) Top: normalized revenue $N(\mathbf{x})/N(\mathbf{x}^{\Gamma=0})$; bottom: violation probability \hat{P} under adversarial shocks (solid) and i.i.d. shocks (dashed), for $\alpha \in \{0.10, 0.20\}$. Revenue cost is below 1% even at $\Gamma = n$; violations vanish by $\Gamma/n \approx 0.05$. (b) 5%-quantile of realized margin vs. Γ/n ; higher α produces a larger margin buffer and higher tail quantile. (c) Heatmap of violation probability (adversarial, $\alpha = 0.10$, log scale): below the diagonal $\Gamma_{\text{attack}} = \Gamma$ (dashed) all cells are white (zero violations, Theorem 2); above the diagonal violations increase smoothly.

6.5 Aggregate summary

Table 1 consolidates representative configurations across scales and uncertainty levels, using $\Gamma = \lfloor \sqrt{n} \rfloor$ throughout. All reported solutions satisfy the robust constraint as certified by (30); adversarial and i.i.d. stress tests at $S = 10\,000$ scenarios show zero or negligible violation rates.

The L_{rd} and $\Delta V_{\text{max}}^{\theta}$ columns are consistent with the additive bound of Proposition 9 on every configuration: the rounding loss stays well below the single-item bound, with ratios $L_{\text{rd}}/\Delta V_{\text{max}}^{\theta}$ ranging from 0.01 to 0.37. The relative gap Gap_{LP} is of order 10^{-5} – 10^{-4} throughout, consistent with the $O(1/n)$ decay established in Section 6.2. Revenue sacrifice is minimal: the revenue ratio $N(\mathbf{x})/N(\mathbf{x}^{\Gamma=0})$ exceeds 0.997 in all cases, indicating that Γ -budget protection costs less than 0.3% of nominal revenue in the representative configurations of Table 1. Runtime scales quadratically in n (roughly 4 s \rightarrow 16 s \rightarrow 65 s \rightarrow 410 s for $n = 50 \rightarrow 500$), consistent with the scaling analysis of Section 6.3.

Table 1: Representative performance across scales (nested prefixes from a single $n = 500$ portfolio, $m = 50$, $\Gamma = \lfloor \sqrt{n} \rfloor$). L_{rd} : absolute round-down loss; $\Delta V_{\text{max}}^\theta$: theoretical additive bound (Proposition 9); Gap_{LP} : $L_{\text{rd}}/\text{OPT}_{\text{LP}}$; Rev. ratio: $N(\mathbf{x})/N(\mathbf{x}^{\Gamma=0})$; Viol. (adv.): \hat{P} under adversarial shocks at $\Gamma_{\text{attack}} = \lfloor 1.5\Gamma \rfloor$; Viol. (iid): \hat{P} under i.i.d. Uniform($-1, 1$) shocks ($S = 10\,000$ scenarios).

n	α	Γ	Time (s)	L_{rd}	$\Delta V_{\text{max}}^\theta$	Gap_{LP}	Rev. ratio	Viol. (adv.)	Viol. (iid)
50	0.10	7	3.79	52.5	547	2.8×10^{-4}	0.998	0	5×10^{-4}
50	0.20	7	3.89	14.4	547	7.8×10^{-5}	0.997	0	2×10^{-3}
100	0.10	10	16.2	72.4	547	2.0×10^{-4}	0.999	0	0
100	0.20	10	15.8	5.08	547	1.4×10^{-5}	0.998	0	5×10^{-4}
200	0.10	14	62.0	25.9	782	3.5×10^{-5}	0.999	0	0
200	0.20	14	68.6	287	782	3.9×10^{-4}	0.998	0	0
500	0.10	22	412	44.4	968	2.3×10^{-5}	0.999	0	0
500	0.20	22	401	92.9	968	4.8×10^{-5}	0.998	0	0

Note: The identical value of 547 for $\Delta V_{\text{max}}^\theta$ at $n = 50$ and $n = 100$ is a direct result of the deterministic nested prefix instance design.

Limitations. Several design choices bound the scope of the experiments above. First, all instances derive from a single synthetic demand model (piecewise-linear with proportional uncertainty) and a single master portfolio; while the generator produces realistic heterogeneity across items, validation on observed pricing data—retail scanner panels, insurance tariffs, or online marketplace catalogs—would test the hull-filtering and rounding machinery under distributional features (e.g. multi-modal demand, correlated perturbations) that the current generator does not produce. Second, the nested-prefix design eliminates cross-instance sampling variation and cleanly isolates the effect of portfolio size, but it means every n -configuration shares the same first n items; independent random instances with multiple replicates would provide complementary evidence on average-case behavior. Third, portfolio sizes are capped at $n = 500$ by the $O(n^2m)$ cost of naïve θ -enumeration (Section 6.3); the sweep-style optimizations of Section 5—restricting candidates to undominated breakpoints and caching hulls incrementally—may extend the practical frontier to $n \geq 10^4$ but are not yet implemented.

7 Stylized Application: Category Pricing in Retail

To illustrate the managerial value of the Γ -budget robust framework beyond the controlled synthetic setting of Section 6, we analyze a stylized retail grocery pricing problem with economically calibrated parameters, non-linear demand, and heterogeneous uncertainty.

Consider a category manager responsible for setting regular (non-promotional) shelf prices for a portfolio of $n = 300$ Stock Keeping Units (SKUs) spanning a mid-size grocery category such as dairy, breakfast, or household cleaning. The manager faces a quarterly gross-margin target Δ dictated by corporate planning, but demand is susceptible to disruptions: unannounced competitor promotions, supply-chain cost shocks, and shifts in consumer preference between national brands and private-label substitutes.

7.1 Economic model and portfolio construction

Portfolio structure. To capture the heterogeneity typical of a grocery category, we partition the 300 SKUs into four segments that reflect standard retail assortment tiers:

1. **Staples** (120 SKUs): high-volume, low-margin essentials (e.g. whole milk, white bread, eggs) with low price sensitivity. Reference prices $a_i \sim \exp(\mathcal{N}(\mu = \log 3.0, \tau^2 = 0.15))$, median $\approx \$3.00$.

2. **Mainstream brands** (100 SKUs): mid-range national-brand products (e.g. branded yogurt, cereal, pasta sauce) with moderate elasticity. Reference prices $a_i \sim \exp(\mathcal{N}(\mu=\log 5.5, \tau^2=0.20))$, median $\approx \$5.50$.
3. **Premium & specialty** (50 SKUs): higher-priced items with larger absolute margins but smaller volume (e.g. organic produce, artisanal cheese, specialty beverages). Reference prices $a_i \sim \exp(\mathcal{N}(\mu=\log 9.0, \tau^2=0.25))$, median $\approx \$9.00$.
4. **Private label** (30 SKUs): store-brand alternatives to mainstream products, positioned on price and highly exposed to competitive price gaps. Reference prices $a_i \sim \exp(\mathcal{N}(\mu=\log 3.5, \tau^2=0.10))$, median $\approx \$3.50$.

Demand model. Consumer response in retail grocery is well described by a constant-elasticity (iso-elastic) demand function with a segment-dependent volume anchor. For each SKU i in segment k , the nominal demand reaction function is

$$\hat{g}_i(x_i) = d_i \left(\frac{x_i}{a_i} \right)^{-\eta_i}, \quad (31)$$

where d_i is the baseline weekly unit volume at reference price a_i and $\eta_i > 1$ is the price elasticity. We draw the segment-specific parameters as follows:

Segment	η_i	d_i	Rationale
Staples	Uniform(1.2, 2.0)	$\exp(\mathcal{N}(\mu=\log 150, \tau^2=0.30))$	inelastic; high turns
Mainstream	Uniform(2.0, 3.5)	$\exp(\mathcal{N}(\mu=\log 60, \tau^2=0.35))$	moderate sensitivity
Premium	Uniform(1.5, 2.5)	$\exp(\mathcal{N}(\mu=\log 20, \tau^2=0.40))$	niche; low volume
Private label	Uniform(3.0, 5.0)	$\exp(\mathcal{N}(\mu=\log 80, \tau^2=0.25))$	price-driven switching

The iso-elastic form (31) generates a revenue curve $r_i(x_i) = x_i \hat{g}_i(x_i) = d_i a_i^{\eta_i} x_i^{1-\eta_i}$ that is concave in x_i when $\eta_i > 1$, but the per-item margin contribution $s_i(x_i) = \omega_i(x_i - \Delta a_i) \hat{g}_i(x_i)$, when evaluated over a discrete menu, need not trace a concave envelope in the cost–value plane, making the upper-hull filtering of Section 4.1 essential.

Exposures and margin target. We set $\omega_i = d_i/\bar{d}$ where \bar{d} is the portfolio mean of d_i , so that the margin constraint weights each SKU by its volume share—reflecting the standard retail practice of measuring category margin on a revenue-weighted basis. The margin target Δ is calibrated to represent a gross-margin hurdle of approximately 30%:

$$\Delta = (1 - 0.02) \frac{\sum_{i=1}^n \omega_i \tilde{x}_i \hat{g}_i(\tilde{x}_i)}{\sum_{i=1}^n \omega_i a_i \hat{g}_i(\tilde{x}_i)},$$

with \tilde{x}_i the menu point closest to a_i . The 2% relative slack (cf. Section 6.1) ensures feasibility across the full Γ -grid; we verify this on all tested configurations.

Discrete price menus. For each SKU i we construct $m = 20$ candidate price points within the admissible band $[(1 - \sigma_i)a_i, (1 + \sigma_i)a_i]$ with $\sigma_i = 0.10$. Rather than spacing prices uniformly, we adopt a retailer-realistic grid that respects psychological price endings: each candidate is rounded to the nearest cent ending in $$.X9$ (i.e. \$2.49, \$3.99, \$5.19, etc.) and then deduplicated. This produces menus with slightly irregular spacing and occasionally fewer than m distinct options for low-priced staples, since a $\pm 10\%$ band around \$3.00 offers less price granularity than the same band around \$9.00.

Demand uncertainty. We model heterogeneous uncertainty that reflects the distinct risk profiles of each segment. The deviation bound is $\delta_i(x_i) = \alpha_i \hat{g}_i(x_i)$, with segment-specific uncertainty levels:

Segment	α_i	Rationale
Staples	0.08	stable demand; low substitution risk
Mainstream	0.15	exposed to promotional warfare
Premium	0.12	niche loyalty; moderate shock exposure
Private label	0.25	high cross-price sensitivity; competitor-driven

This heterogeneity is important: a uniform α would understate risk for price-sensitive private-label SKUs and overstate it for inelastic staples. Under the Γ -budget model, the adversary selects the *most damaging* Γ items to perturb, so high- α_i SKUs with large margin contributions become the natural attack surface. The theoretical guarantees of [Theorem 2](#) and [Proposition 9](#) hold for any parameter realization; only the magnitude of the revenue–risk tradeoff depends on the specific instance.

7.2 Experimental design

We generate the $n = 300$ portfolio from a single seed (master seed 42) and solve the robust MCKP at

$$\Gamma \in \{0, 1, 5, 10, 15, \lfloor \sqrt{n} \rfloor = 17, 30, 50, 75, 100, n\}$$

using [Algorithm 1](#). For each Γ -level we record the nominal objective, wall-clock time, rounding loss L_{rd} , and the number of SKUs whose optimal price shifts relative to the $\Gamma = 0$ solution. Each solution is stress-tested with $S = 10\,000$ Monte Carlo scenarios under both the adversarial and i.i.d. perturbation protocols defined in [Section 6.4](#), with $\Gamma_{\text{attack}} \in \{\Gamma, \lfloor 1.5\Gamma \rfloor, 2\Gamma, n\}$.

7.3 Managerial insights

Concentration risk under nominal pricing. When optimizing nominally ($\Gamma = 0$), the MCKP fulfills the category margin target by extracting surplus from a concentrated subset of inelastic items. In the generated instance, of the 300 SKUs only 68 have non-trivial margin contributions (above the 25th percentile of positive contributions)—predominantly staples and a handful of premium items that are upgraded above their reference price. This pricing architecture is mathematically optimal under perfect demand foresight but creates a fragile margin structure: the top- Γ contributors account for a disproportionate share of the margin surplus, so even a modest number of simultaneous demand shocks can breach the category target.

Under i.i.d. stochastic shocks ($\xi_i \sim \text{Uniform}(-1, 1)$ independently for all 300 items), the nominal solution already exhibits a violation rate of approximately 50% (a coincidence distinct from the 50% adversarial rate observed in [Section 6.4](#), driven here by heterogeneous uncertainty profiles)—the margin target is breached in half of all scenarios. Under worst-case-direction adversarial shocks at $\Gamma_{\text{attack}} = n$, the violation rate reaches 100%. These numbers underscore that the nominal solution, while revenue-optimal, is operationally unacceptable for a category manager facing any demand uncertainty.

Structural diversification under Γ -protection. Applying the robust algorithm with a modest budget ($\Gamma = 17 \approx \lfloor \sqrt{n} \rfloor$, protecting against simultaneous shocks to roughly 6% of the portfolio) produces a qualitatively different pricing architecture ([Figure 4b](#)). The robust solution:

- *Spreads margin contributions* across a broader base: the number of SKUs with non-trivial margin contribution increases from 68 to 76 (12% increase) relative to the nominal solution;
- *Moderates prices on high-exposure items*: 39 of 300 SKUs shift price relative to the nominal solution, with private-label SKUs—which carry the largest per-unit uncertainty ($\alpha_i = 0.25$)—seeing the largest downward adjustments, reducing their individual contribution to worst-case margin loss;

- *Preserves nearly all nominal revenue:* the revenue sacrifice is 0.28% of the $\Gamma = 0$ objective, well within the noise of typical weekly demand fluctuations.

This illustrates the core managerial tradeoff of the Γ -budget approach: by sacrificing a fraction of a percent of expected revenue, the category manager structurally diversifies margin risk away from a concentrated set of vulnerable SKUs.

Guidance on choosing Γ in practice. The budget parameter Γ controls the number of simultaneous worst-case demand deviations the solution must withstand. Bertsimas and Sim (2004) show that if individual deviations are independent and symmetrically distributed, the probability that more than Γ items simultaneously reach their worst case is bounded above by a quantity that decays exponentially in Γ^2/n . For the 300-SKU portfolio, $\Gamma = 17 \approx \lfloor \sqrt{n} \rfloor$ already provides a nontrivial level of probabilistic coverage under this bound. In practice, calibration should still be guided by historical demand data and scenario analysis, since the Bertsimas–Sim bound is conservative and the stress tests considered here are stylized. A category manager can calibrate Γ empirically by examining historical demand data: if past records show that at most K SKUs have simultaneously experienced demand drops exceeding one standard error of the demand estimate in any given week, then setting $\Gamma \geq K$ provides an empirically grounded protection level. The revenue–risk frontier in Figure 4(a) supports this calibration by visualizing the marginal revenue cost of each additional unit of Γ , allowing the manager to select the point on the frontier that best balances revenue performance against margin-breach risk tolerance.

Effectiveness of protection. Figure 4a displays the revenue–risk frontier as two vertically aligned panels. The top panel shows that the cost of robustness is remarkably small: even full box protection ($\Gamma = n = 300$) sacrifices less than 0.7% of nominal revenue in the stylized retail case study. The bottom panel shows violation probability under adversarial and i.i.d. shocks. Under i.i.d. shocks, the 51% violation rate of the nominal solution drops below 0.2% at $\Gamma = 5$ (i.e. $\Gamma/n \approx 0.02$) and to zero for $\Gamma \geq 10$. Under adversarial shocks at $\Gamma_{\text{attack}} = \lfloor 1.5\Gamma \rfloor$ (strictly exceeding the protection budget for $\Gamma > 0$), the observed violation rate is zero for all $\Gamma \geq 1$, indicating that even minimal protection eliminates all observed adversarial violations at moderate over-attack levels.

At the matching attack level ($\Gamma_{\text{attack}} = \Gamma$), all 10 000 adversarial scenarios produce zero observed violations for every tested Γ , consistent with the certificate of Theorem 2 and serving as an end-to-end correctness check.

Rounding-loss guarantee. The rounding loss satisfies $L_{\text{rd}} < \Delta V_{\text{max}}^\theta$ on every configuration, with a ratio $L_{\text{rd}}/\Delta V_{\text{max}}^\theta = 0.023$ at $\Gamma = \lfloor \sqrt{n} \rfloor$, consistent with the bound in Proposition 9 for this non-linear iso-elastic demand setting.

Operational practicality. Algorithm 1 solves the $n = 300$, $m = 20$ instance in approximately 18 seconds for the tested Γ -values. While not instantaneous, this runtime is compatible with periodic repricing workflows such as weekly or batch updates when cost files or demand estimates are refreshed. Sweep-style optimizations of the type discussed in Section 5 may reduce runtime further, but these improvements are not yet implemented here.

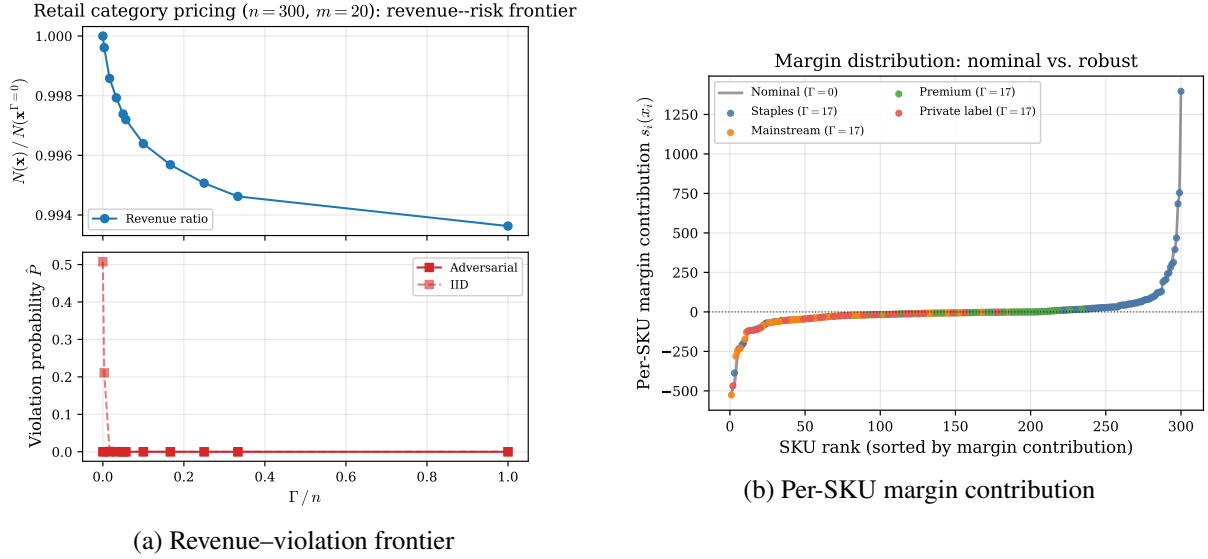


Figure 4: Retail category pricing ($n = 300, m = 20$, heterogeneous α_i). (a) Top: normalized category revenue $N(\mathbf{x})/N(\mathbf{x}^{\Gamma=0})$; bottom: violation probability \hat{P} under adversarial shocks at $\Gamma_{\text{attack}} = \lfloor 1.5\Gamma \rfloor$ (solid) and i.i.d. shocks (dashed). Revenue cost is below 0.7% even at $\Gamma = n$; i.i.d. violations vanish by $\Gamma/n \approx 0.03$. (b) Sorted per-SKU margin contribution $s_i(x_i)$ for the nominal solution ($\Gamma = 0$, gray) and the robust solution ($\Gamma = 17 \approx \lfloor \sqrt{n} \rfloor$, colored by segment). The robust solution compresses the right tail and spreads positive contributions across a broader SKU base.

8 Conclusion

We have studied discrete pricing under demand uncertainty through the lens of robust optimization, reducing the problem to a multiple-choice knapsack problem with a Γ -budget uncertainty set in the capacity constraint. Three main contributions emerge from this reduction.

First, we established that the LP relaxation of the fixed- θ subproblem admits an additive integrality gap bounded by a single item’s maximum hull-value jump ΔV_{\max}^{θ} (Proposition 9). Under the boundedness and linear-growth assumptions of Corollary 10, this yields a relative gap that decays as $O(1/n)$.

Second, we showed that the Γ -budget robust constraint admits an exact reformulation via θ -enumeration over a finite set of breakpoints (Theorem 6 and Proposition 7), preserving the combinatorial structure that makes the hull-greedy approach applicable. The resulting procedure avoids relying on a generic integer-programming solver in its main loop and exhibits close-to- $O(n^2m)$ empirical scaling on the instances tested.

Third, numerical experiments on nested synthetic portfolios (n up to 500, m up to 100) and a stylized retail application ($n = 300$ SKUs, four segments, heterogeneous uncertainty) are consistent with these theoretical properties on the tested instances. Across these experiments, the observed integrality gap is negligible, Γ -budget protection reduces or eliminates observed margin violations at a revenue cost below 1% in the synthetic frontier experiment and in the stylized retail case study, and the algorithm solves the reported instances in seconds to minutes.

Several directions remain open. Implementing the sweep-style optimizations of Section 5—restricting θ -candidates to undominated breakpoints and caching hulls incrementally—may reduce runtime by one to two orders of magnitude, making portfolios with $n \geq 10^4$ items tractable. Extending the uncertainty model to capture cross-item demand correlations (e.g. through factor-based or ellipsoidal sets) would broaden applicability to settings where substitution effects dominate. A natural starting point is a factor model $\delta_i(x_i) = \bar{\delta}_i(x_i) + \beta_i \zeta$ where ζ is a common shock and β_i are factor loadings; the resulting uncertainty set is an intersection of a Γ -budget set with an ellipsoidal constraint, and the parametric decomposition of Theorem 6 may admit an extension to this setting via a higher-dimensional dual representation. Validation on observed transaction-level pricing data remains an important next step.

Data and Code Availability

To facilitate reproducibility, the solver implementation and the code used to generate the reported numerical experiments are publicly available on GitHub:

https://github.com/eric939/robust_mckp

Acknowledgments. The author thanks Prof. Dr. Angela Kunoth (Department of Mathematics, University of Cologne) for her guidance and support. The problem was posed by Dr. Christian Mollet (Hannoversche Versicherung, Hannover, Germany), and the author also thanks him and his colleagues for several helpful discussions.

References

- Ben-Tal, A. and Nemirovski, A. (1999). Robust solutions of uncertain linear programs. *Operations Research Letters*, 25(1), 1–13. [https://doi.org/10.1016/S0167-6377\(99\)00016-4](https://doi.org/10.1016/S0167-6377(99)00016-4).
- Bertsimas, D. and Sim, M. (2004). The price of robustness. *Operations Research*, 52(1), 35–53. <https://doi.org/10.1287/opre.1030.0065>.
- Boukhari, S. and Hifi, M. (2023). An exact algorithm for the multiple-choice knapsack problem with setups. *Computers & Industrial Engineering*, 188, 109818. <https://doi.org/10.1016/j.cie.2023.109818>.
- Boukhari, S. and Hifi, M. (2024). Combining local branching and descent method for solving the multiple-choice knapsack problem with setups. *International Transactions in Operational Research*, 31(1), 29–52. <https://doi.org/10.1111/itor.13326>.
- Caserta, M. and Voß, S. (2019). The robust multiple-choice multidimensional knapsack problem. *Omega*, 86, 16–27. <https://doi.org/10.1016/j.omega.2018.06.014>.
- Dyer, M. E. (1984). An $O(n)$ algorithm for the multiple-choice knapsack linear program. *Mathematical Programming*, 29(1), 57–63. <https://doi.org/10.1007/BF02592083>.
- Goerigk, M., Lendl, S., and Wulf, L. (2021). Robust combinatorial optimization with locally budgeted uncertainty. *Open Journal of Mathematical Optimization*, 2, Article 3. <https://doi.org/10.5802/ojmo.5>.
- Hamzeei, M., Lim, A., and Xu, J. (2022). Robust price optimization of multiple products under interval uncertainties. *Journal of Revenue and Pricing Management*, 21(4), 442–454. <https://doi.org/10.1057/s41272-021-00351-w>.
- Ibaraki, T., Hasegawa, T., Teranaka, K., and Iwase, J. (1978). The multiple-choice knapsack problem. *Journal of the Operations Research Society of Japan*, 21(1), 59–95. <https://doi.org/10.15807/jorsj.21.59>.
- Kellerer, H., Pferschy, U., and Pisinger, D. (2004). *Knapsack Problems*. Springer.
- Monaci, M., Pferschy, U., and Serafini, P. (2013). Exact solution of the robust knapsack problem. *Computers & Operations Research*, 40(11), 2625–2631. <https://doi.org/10.1016/j.cor.2013.05.005>.
- Nauss, R. M. (1978). The 0–1 knapsack problem with multiple choice constraints. *European Journal of Operational Research*, 2(2), 125–131. [https://doi.org/10.1016/0377-2217\(78\)90108-X](https://doi.org/10.1016/0377-2217(78)90108-X).
- Pisinger, D. (1995). A minimal algorithm for the multiple-choice knapsack problem. *European Journal of Operational Research*, 83(2), 394–410. [https://doi.org/10.1016/0377-2217\(95\)00015-I](https://doi.org/10.1016/0377-2217(95)00015-I).
- Sinha, P. and Zoltners, A. A. (1979). The multiple-choice knapsack problem. *Operations Research*, 27(3), 503–515. <https://doi.org/10.1287/opre.27.3.503>.

A Knapsack Problem

Classical 0–1 Knapsack. Given items $i = 1, \dots, n$ with value $v_i \geq 0$ and cost $c_i \geq 0$, and a capacity C , the 0–1 knapsack problem is

$$\max \sum_{i=1}^n v_i y_i \quad (32)$$

$$\text{s.t.} \quad \sum_{i=1}^n c_i y_i \leq C, \quad (33)$$

$$y_i \in \{0, 1\} \quad (i = 1, \dots, n). \quad (34)$$

Multiple-Choice Knapsack (MCKP). This problem was first introduced by [Nauss \(1978\)](#) as a generalization of the classical knapsack problem. Items are partitioned into n groups; from each group exactly one option must be chosen. Let group i have discrete options (price levels) indexed by j , with value v_{ij} and cost c_{ij} . With capacity C , the MCKP is

$$\max \sum_{i=1}^n \sum_j v_{ij} z_{ij} \quad (35)$$

$$\text{s.t.} \quad \sum_{i=1}^n \sum_j c_{ij} z_{ij} \leq C, \quad (36)$$

$$\sum_j z_{ij} = 1 \quad (i = 1, \dots, n), \quad (37)$$

$$z_{ij} \in \{0, 1\} \quad (\forall i, j). \quad (38)$$

B Proof of the Main Structural Theorem, Steps 1–3

We provide the first three steps of the proof of [Theorem 5](#) for completeness. These arguments are standard; we include them because our notation differs from prior sources.

Step 1: Convex-hull reformulation. Fix an item i . For any feasible vector $(z_{ij})_{j=1}^m$ with $\sum_j z_{ij} = 1$ and $z_{ij} \geq 0$, define

$$(c_i, v_i) := \left(\sum_{j=1}^m c_{ij} z_{ij}, \sum_{j=1}^m v_{ij} z_{ij} \right).$$

Then $(c_i, v_i) \in \text{conv}(\mathcal{P}_i)$ by definition of convex hull, since it is a convex combination of points in \mathcal{P}_i . Conversely, every point in $\text{conv}(\mathcal{P}_i)$ admits such a representation as a convex combination of points in \mathcal{P}_i . Therefore, (17) is equivalent to choosing $(c_i, v_i) \in \text{conv}(\mathcal{P}_i)$ for all i to maximize $\sum_i v_i$ subject to $\sum_i c_i \leq C$.

Step 2: Restriction to the upper hull (proof of (i)). Fix i and a feasible solution with induced $(c_i, v_i) \in \text{conv}(\mathcal{P}_i)$. Consider the set

$$U_i(c) := \sup\{v : (c, v) \in \text{conv}(\mathcal{P}_i)\}.$$

Since $\text{conv}(\mathcal{P}_i)$ is a compact polytope, the supremum is attained and $U_i(c)$ describes the upper hull of $\text{conv}(\mathcal{P}_i)$. Let $v'_i := U_i(c_i)$. Then $(c_i, v'_i) \in \text{conv}(\mathcal{P}_i)$, and $v'_i \geq v_i$ by construction. Replacing (c_i, v_i) by (c_i, v'_i) for each i preserves feasibility of $\sum_i c_i \leq C$ and weakly increases the objective. Hence there exists an optimal solution with each (c_i, v_i) on the upper hull.

The upper hull of a polytope in \mathbb{R}^2 is a polyline connecting consecutive vertices of \mathcal{H}_i . Thus, if (c_i, v_i) lies on the hull and $c_i \in [c_{i,k}^H, c_{i,k+1}^H]$ for some k , then (c_i, v_i) is a convex combination of the two adjacent vertices $(c_{i,k}^H, v_{i,k}^H)$ and $(c_{i,k+1}^H, v_{i,k+1}^H)$. This proves (i).

Step 3: Segment-length parameterization (proof of (ii)). Fix an item i and let the upper-hull vertices of $\text{conv}(\mathcal{P}_i)$ be

$$\mathcal{H}_i = \{(c_{i,1}^H, v_{i,1}^H), \dots, (c_{i,p_i}^H, v_{i,p_i}^H)\}, \quad c_{i,1}^H < \dots < c_{i,p_i}^H.$$

For $k = 1, \dots, p_i - 1$ define

$$\Delta c_{i,k}^H := c_{i,k+1}^H - c_{i,k}^H > 0, \quad \rho_{i,k}^H := \frac{v_{i,k+1}^H - v_{i,k}^H}{\Delta c_{i,k}^H}.$$

Every point (c_i, v_i) on the upper hull lies on a unique segment between adjacent vertices, so there exist $k^* \in \{1, \dots, p_i - 1\}$ and $\alpha \in [0, 1]$ such that

$$(c_i, v_i) = (1 - \alpha)(c_{i,k^*}^H, v_{i,k^*}^H) + \alpha(c_{i,k^*+1}^H, v_{i,k^*+1}^H).$$

Define segment-length variables $\ell_{i,k}$ by

$$\ell_{i,k} := \begin{cases} \Delta c_{i,k}^H, & k < k^*, \\ \alpha \Delta c_{i,k^*}^H, & k = k^*, \\ 0, & k > k^*, \end{cases} \quad \text{so that} \quad 0 \leq \ell_{i,k} \leq \Delta c_{i,k}^H.$$

Then the identities

$$c_i = c_{i,1}^H + \sum_{k=1}^{p_i-1} \ell_{i,k}, \quad v_i = v_{i,1}^H + \sum_{k=1}^{p_i-1} \rho_{i,k}^H \ell_{i,k}$$

hold, since on each segment k the increase in v equals $\rho_{i,k}^H$ times the increase in c . Summing these expressions over i and substituting into the convex-hull formulation from Step 1 yields

$$\max \sum_{i=1}^n \left(v_{i,1}^H + \sum_{k=1}^{p_i-1} \rho_{i,k}^H \ell_{i,k} \right) \quad \text{s.t.} \quad \sum_{i=1}^n \left(c_{i,1}^H + \sum_{k=1}^{p_i-1} \ell_{i,k} \right) \leq C, \quad 0 \leq \ell_{i,k} \leq \Delta c_{i,k}^H.$$

Dropping the constant $\sum_i v_{i,1}^H$ in the objective and moving $\sum_i c_{i,1}^H$ to the right-hand side of the capacity constraint gives (18), proving (ii).